EUROPEAN COMMISSION
Community Research

RAPHAEL

Contract Number: 516508 (FI6O)

DELIVERABLE (DCP1.1)
AVR benchmark definition report

Author(s): **W. Bernnat..............................**
H. Werner..............................

Reporting period: e.g. 15/04/2005– 15/04/2006

Date of issue of this report : 07/04/2006

Start date of project : **15/04/2005** Duration : **48 Months**

Project co-funded by the European Commission under the Euratom Research and Training Programme on Nuclear Energy within the Sixth Framework Programme (2002-2006)		
Dissemination Level		
PU	Public	
RE	Restricted to the partners of the RAPHAEL project	X
CO	Confidential, only for specific distribution list defined on this document	

Distribution list

Person and organisation name and/or group	Comments

ReActor for Process heat, Hydrogen And ELectricity generation (RAPHAEL)		
Sub-project: SP-CP **Work package:** 1	**RAPHAEL document no:** RAPHAEL-0607-D-CP1.1	**Document type:** D=Deliverable / M=Minute / P=Progress report / S=Support
Issued by: USTUTT IKE (D) **Internal no.:** N/A		**Document status:** Review

Document title
AVR benchmark definition report
Executive summary

The AVR is a High Temperature Reactor, built as an experiment on industrial scale in Jülich, Germany. The main features are a high coolant temperature, pebble fuel in a core with continuous fuel circulation and Helium coolant. The reactor had 21 years of successful power operation and was used as a test bed for various fuel and refuelling strategies. The following experiments performed at AVR:

- Steady state physical experiments
- Dynamic physical experiments
- Hot temperature coefficient
- Simulation of loss of coolant accident

will be described in detail as benchmark exercises to get a data base for validation of transient coupled neutronics and thermal hydraulics codes. For these experiments the burn up dependant core configuration and initial conditions for the different transients were calculated with the HTR-2000 system from H. Werner, FZJ and can be used from the benchmark participants. The experimental results will be prepared by P. Pohl from AVR.

Revisions

Rev.	Date	Short description	Author	WP Leader	SP Leader	Coordinator
00	06/04/2006	First issue	Bernnat USTUTT IKE	Bernnat, USTUTT IKE *signature*	Van Heek, NRG *Signature*	Bogusch, FANP *Signature*
01	2006-11-21	Completion	Bernnat			

Contents

List of figures

List of tables

Appendix

1 AVR benchmark definition

1.1 Introduction

The AVR is a High Temperature Reactor, built as an experiment on industrial scale in Jülich, Germany. The main features are a high coolant temperature, pebble fuel in a core with continuous fuel circulation and Helium coolant. The reactor had 21 years of successful power operation and was used as a test bed for various fuel and refuelling strategies.

An extensive experimental programme was performed with the AVR, especially:

- Steady state physical experiments
- Dynamic physical experiments
- Hot temperature coefficient
- Simulation of loss of coolant accident
- Determination of maximum gas temperature

In view of possible benchmark exercises the following four are the most beneficial, and at the same time very challenging ones.

1 **The so-called "Vierstabklemm-Versuch"** was actually 2 experiments in one. The first consisted in interrupting the forced cooling resulting in reactor shut-down and the change-over from the forced-convection to the natural-heat-dissipation temperature profiles, and the second – with the shut-down rods left withdrawn – in the re-criticality and power development under natural heat dissipation conditions.

2 **The LOCA simulation experiment** incorporated stationary reactor operation at depressurised conditions followed by a similar temperature profile change-over as in (1). A comprehensive set of data was obtained.

3 **The dynamic experiments** with quick changes of the coolant circulator speed or the shut-down rod positions were especially carried out to test reactor dynamics models. The data are well recorded.

4 **The melt-wire experiment** at normal operation is probably the most important of all. Although only stationary, the prediction of the temperature profile of the coolant as exiting from the pebble bed is highly demanding.

For the four mentioned experiments the measured data were well documented and are available from AVR (responsible: Peter Pohl) for comparisons with corresponding calculations. Since the experiments were performed at different times with various reloading schemes, the burn-up distribution and the core composition is difficult to calculate by means of core calculations regarding every reload step performed until the time point of the transient. Therefore, the initial core compositions for the mentioned experiments will be calculated by the validated HTR-2000 system by FZJ (Dr. Werner) and delivered to the RAPHAEL partners. Using these data, the geometrical description of the AVR and the stationary or transient initial and boundary conditions the participants of these benchmarks can proof their tools for HTR pebble bed reactor analysis for stationary and transient coupled neutronics and thermal-hydraulics problems. There are many documents available concerning the description of AVR and the AVR experiments. A comprehensive compilation about AVR is integrated into the "International Reactor Physics Experiment Evaluation Handbook" of the OECD/NEA data bank [1]. Furthermore, there exists a textbook: "AVR-Experimental High-Temperature Reactor - 21 Years of Successful Operation for a Future Energy Technology" [2] which gives a good overview over the AVR reactor and the operational experience.

2 Selection of transient experiments for benchmarking

2.1 Simulation of a loss of coolant (LOCA) accident (October 1988)

In October 1988 the main experiment for the simulation of a loss of coolant accident was performed. The purpose of the test was to simulate the conditions of a loss-of-coolant accident as realistically as possible. At AVR a fast depressurisation of the primary system was impossible because of contamination of the gas. Therefore, the cooling gas could only be pumped off into the storage vessel via the gas purification system, which lasted about three days. After three days, however, the decay heat level is substantially lower than in a loss of coolant event e. g. expected after a break of a line of the main primary loop. Therefore, the decay heat was simulated by corresponding fission power generation controlled by operator.
The experiment was performed by following steps:

- The reactivity was dropped by stop of recirculation of pebbles and the shutdown rods were therefore only slightly inserted.
- Then the reactor was shut down and the cooling gas pressure lowered to 1 bar.
- To get the real starting conditions for LOCA the reactor was operated for some days at low power until the full load temperatures were reached.
- During the actual simulation of the accident the decay heat curve for full load conditions was simulated with fission power, controlled via the shutdown rods.

During the simulation of the accident the temperatures in the core zone and the surrounding metallic internals were recorded for some days.

2.2 Dynamic experiments with power transients by movement of control rods variation of mass flow

From March 1st until March 5th 1988 a series of dynamic experiments were performed for a core with comparable much LEU fuel elements. Following experiments were performed

- Reduction of mass flow to 50% and return to 100%
- Insertion of control rods
- Reduction of mass flow to 80% and subsequent Xe-transient

The reactor was operated from January to End of February 1988 with constant full power and 810°C, interrupted by a short shutdown interval from 21st to 25th February 1988. One day before the first experiment the He exit temperature was lowered at full power from 810 to 775 °C to be able to start all following experiments at identical temperature.

3 Description of the AVR facility

The AVR reactor is a high temperature reactor with pebble bed core. The complete reactor system is shown in Figures 1 and 2. The main design data are given in Table 1. A vertical and horizontal sections through the core (including RPV) shows Fig. 3. Fig. 4 and Fig.5 show vertical and horizontal sections through the core. From Fig. 5 one can see that the core is not rotationally symmetrical due to the so called graphite noses in which the four control rods can be moved. This noses are also illustrated by Fig. 6, a view into the empty AVR core.

The reactor is loaded with pebbles of graphite with a spherical shape (6 cm diameter) inside the pebbles there is a fuel zone (matrix zone) of 5 cm diameter which contains the fuel in form of coated particles (see Fig. 7). The different fuel element types will be described together in the chapter describing the initial conditions before the experiments. More details can be seen from [1] and [2]. The description of the experiments are reported originally in the AVR reports "AVR dynamic experiments till 1988" , (Pohl 1990) and " AVR LOCA simulation data" (Pohl, 1989).

Table 1: Main data for the AVR

AVR Experimental Nuclear Power plant		
Main Data		
Thermal power		46 MW
Electrical output		15 MW
Core:	Diameter	3.0 m
	Height	2.8 m
Power density		2.6 MW/m^3
Fuel:	Composition	HEU/Thorium or LEU (10 %; 17 %)
	Arrangement	pebble bed 92,000 pebbles
	Discharge burn-up	112 % fifa 18.2 % fima, 162 GWd/to
	Max. temperature	> 1350 °C
Coolant:	Pressure	11 bar
	Inlet temperature	275 °C
	Outlet temperature	950 °C

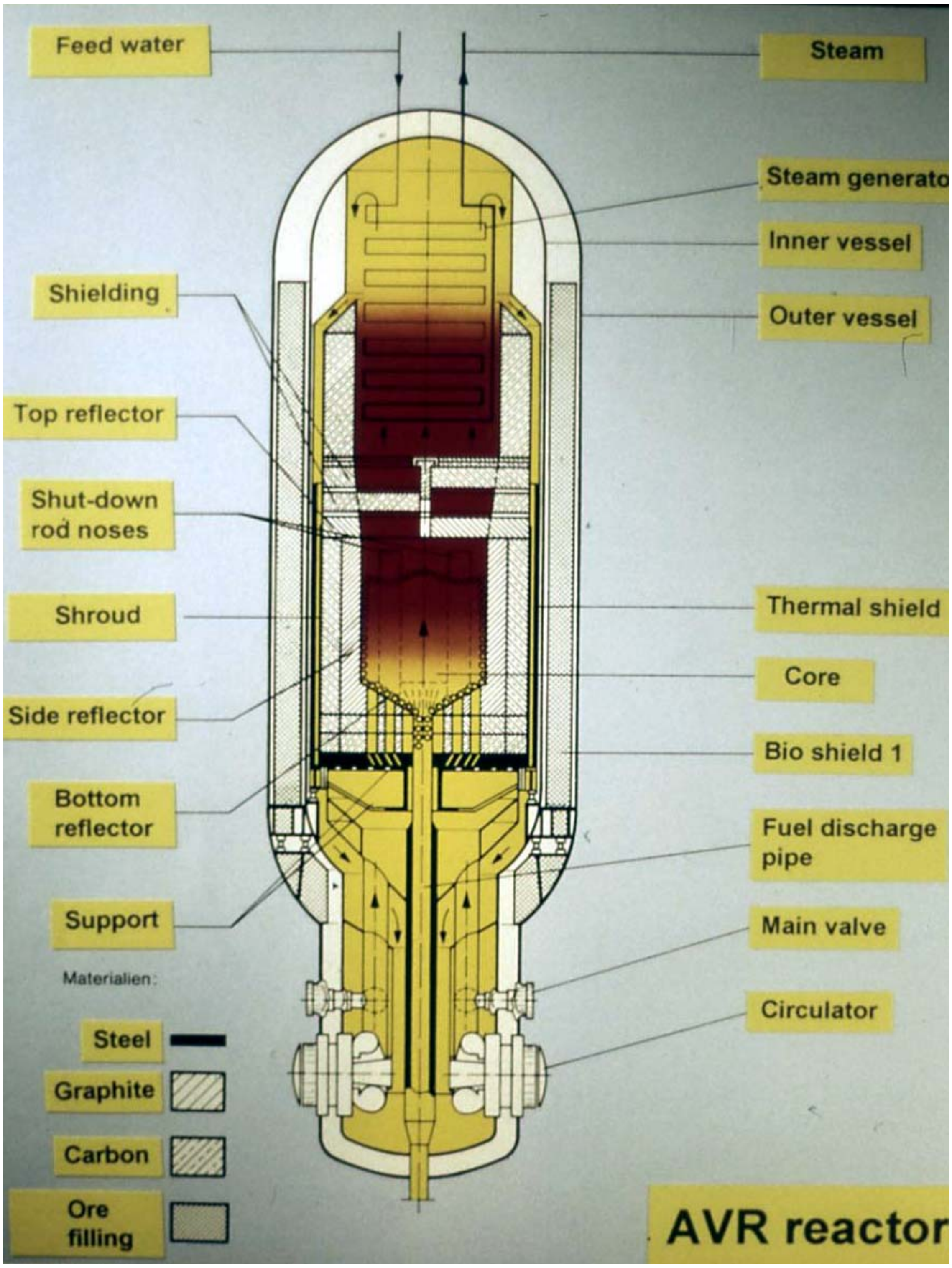

Figure 1: vertical section through AVR reactor design

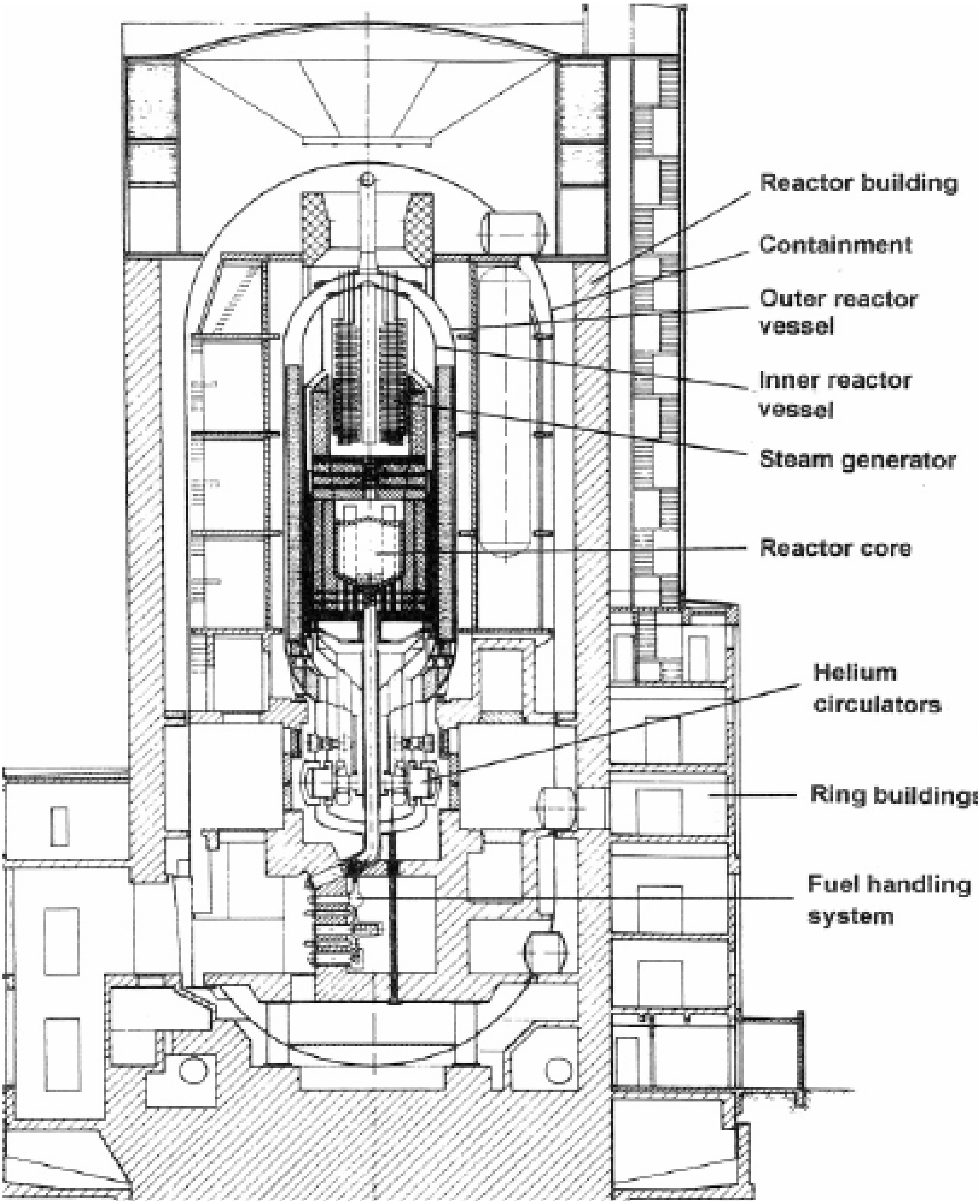

Figure 2: Vertical section through AVR reactor and building

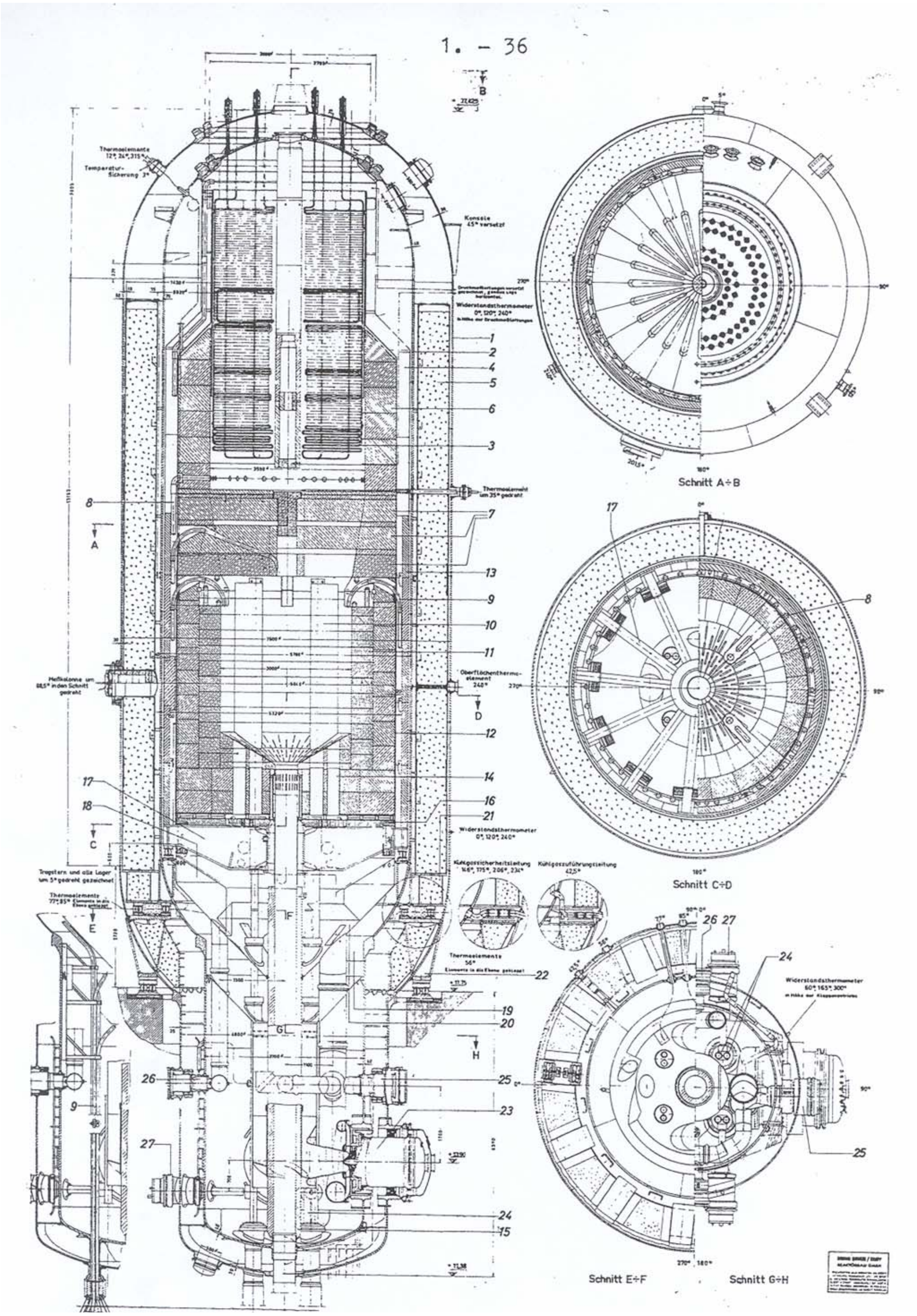

Figure 3: Vertical and horizontal sections through AVR core and RPV

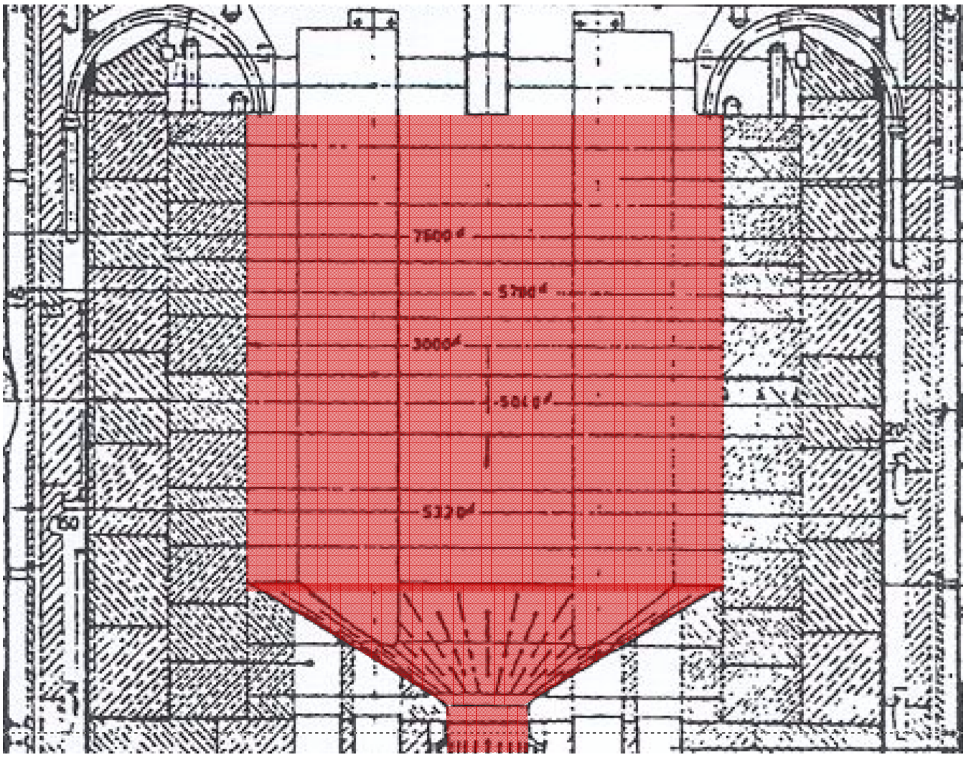

Figure 4: Vertical section through AVR core and reflector

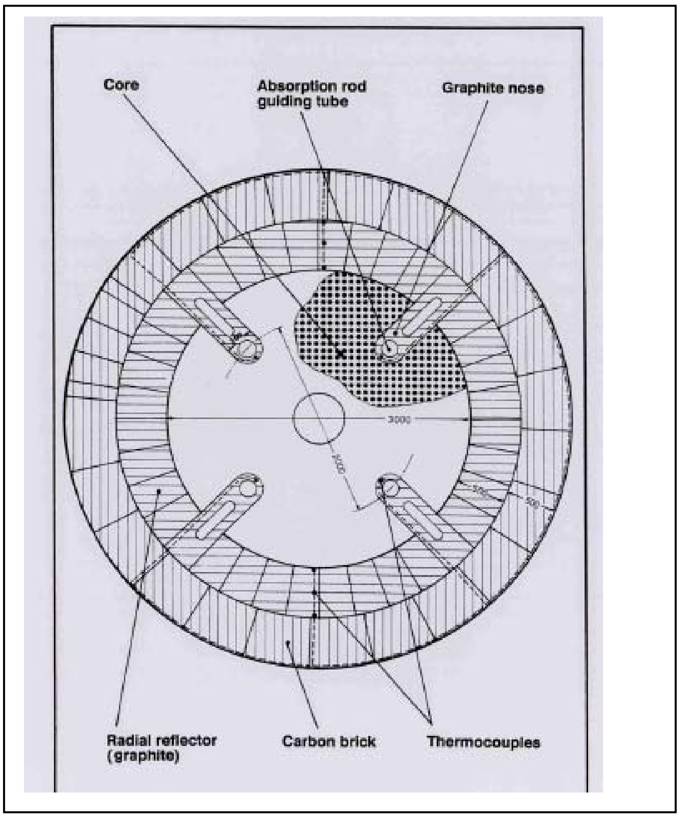

Figure 5: Horizontal section through AVR core

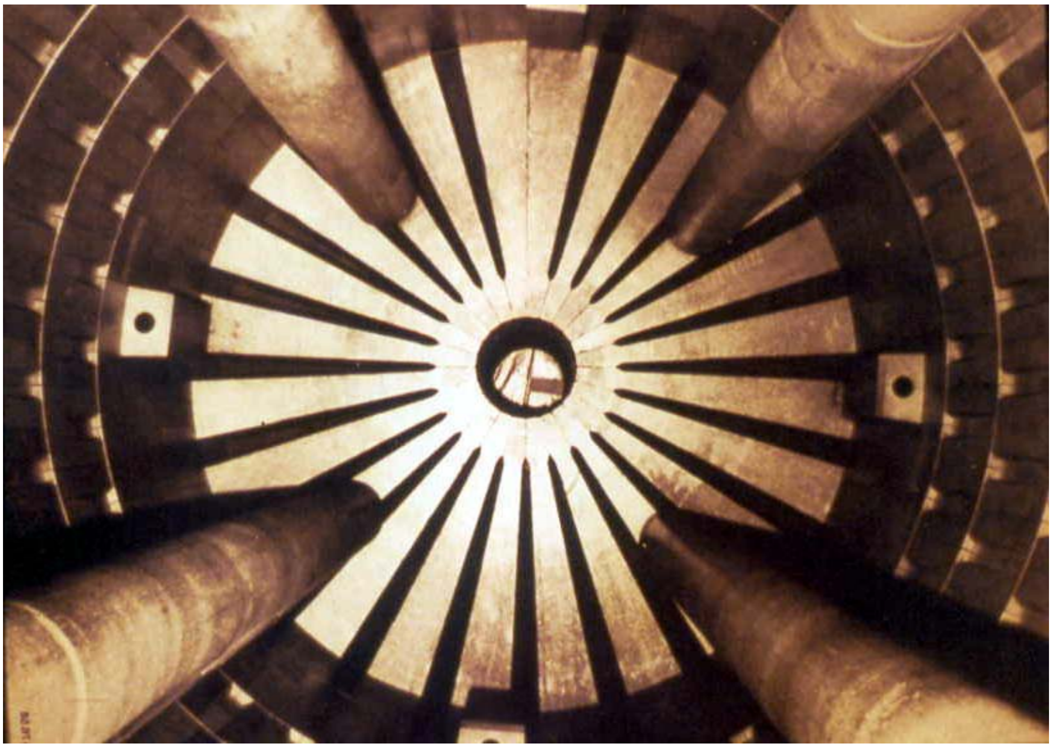

Figure 6: View into empty AVR core

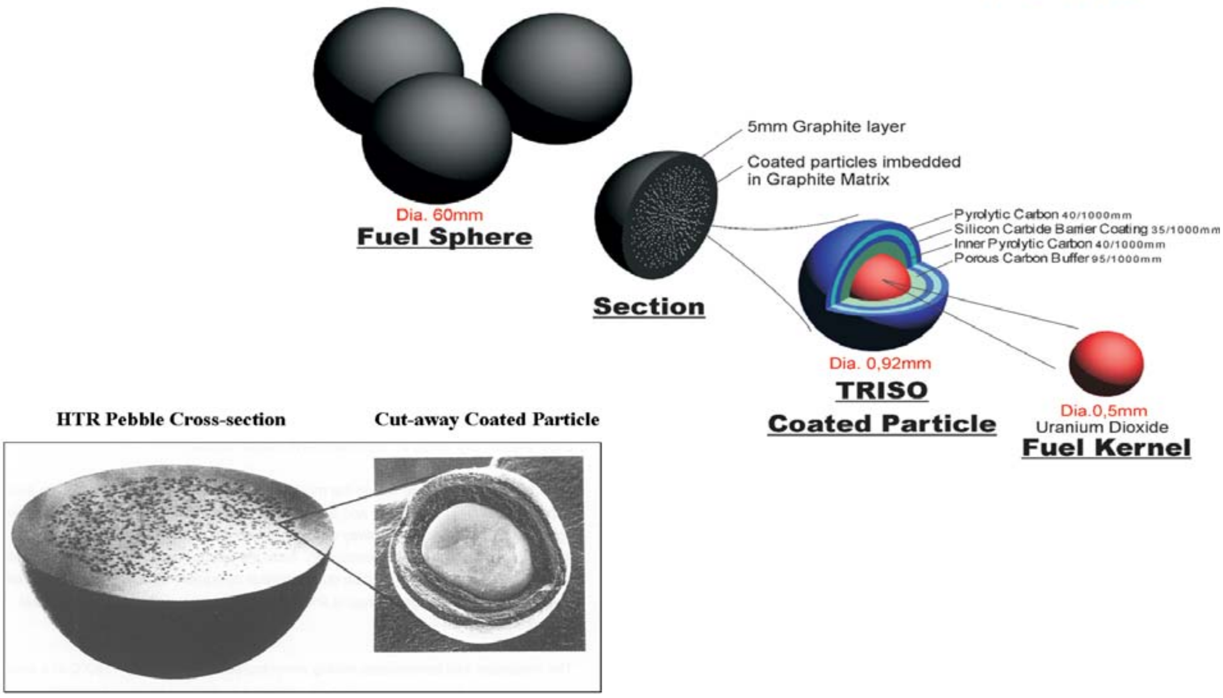

Figure 7: HTR Pebble with TRISO particles

4 Data base for benchmark calculations

4.1 Core model

The core of AVR consists of pebbles filled into a cylindrical graphite reflected cavity (see corresponding Figures). The bottom of the core is a cone. The control rods are moved in graphite noses inside the core cylinder. The pebbles flow in several (9) channels with distinct velocity. This is described by Fig. 8. To regard the flowing pebbles, the core is subdivided into many regions which contain several (up to 50) classes of fuel assemblies (different types, different burnup due to recycling). Fig. 9 shows the typical modelling of the AVR core (incl. Reflector). The zones in Fig. 9 are described by following Tab. 2.

Table 2: Description of zones for AVR calculation (see Fig. 9)

Z1-25	Corezonen	core zones
TK26	Top Reflektor Kohlestein	top reflector carbon
TR27	Top Reflektor Grafit	top reflector graphite
HO28	Hohlraum	cavity
SR29	Seiten Reflektor Grafit	side reflector graphite
SK30	Seiten Reflektor Kohlestein	side reflector carbon
BR31	Boden Reflektor Grafit	bottom reflector graphite
KA32	Kugel Abzug Rohr	pebble discharge tube
BK33	Boden Reflektor Kohlestein (mit Bor)	bottom reflector(boron)
BK34	Boden Reflektor Kohlestein	bottom reflector(carbon)
NA35	Nasen Grafit	graphite nose
NA36	Nasen Grafit	graphite nose
AS37	Abschaltstab (Randbedingungen)	shutdown rod
HS38	Hohlraum Abschaltstab	cavity shutdown rod
RS39	Reaktor Schalung (Stahl)	barrel (steel)
TS40	Thermischer Schild (Stahl)	thermal shield (steel)
IB41	Innerer Behälter (Stahl)	inner container (steel)
SB42	Schutz Behälter (Stahl)	protection container (steel)
BS43	Biologischer Schild (mixture 80% Fe)	Biological shield
AM44	Abschirm Mantel (Blei)	shield (lead)
SK45	Seiten Reflektor Kohlestein	side reflector carbon
SR46	Seiten Reflektor Grafit	side reflector graphite
SR47	Seiten Reflektor Grafit	side reflector graphite
SR48	Seiten Reflektor Grafit	” ”
SR49	Seiten Reflektor Grafit	” ”
SK50	Seiten Reflektor Kohlestein	side reflector carbon
SK51	Seiten Reflektor Kohlestein	side reflector carbon
SK52	Seiten Reflektor Kohlestein	side reflector carbon

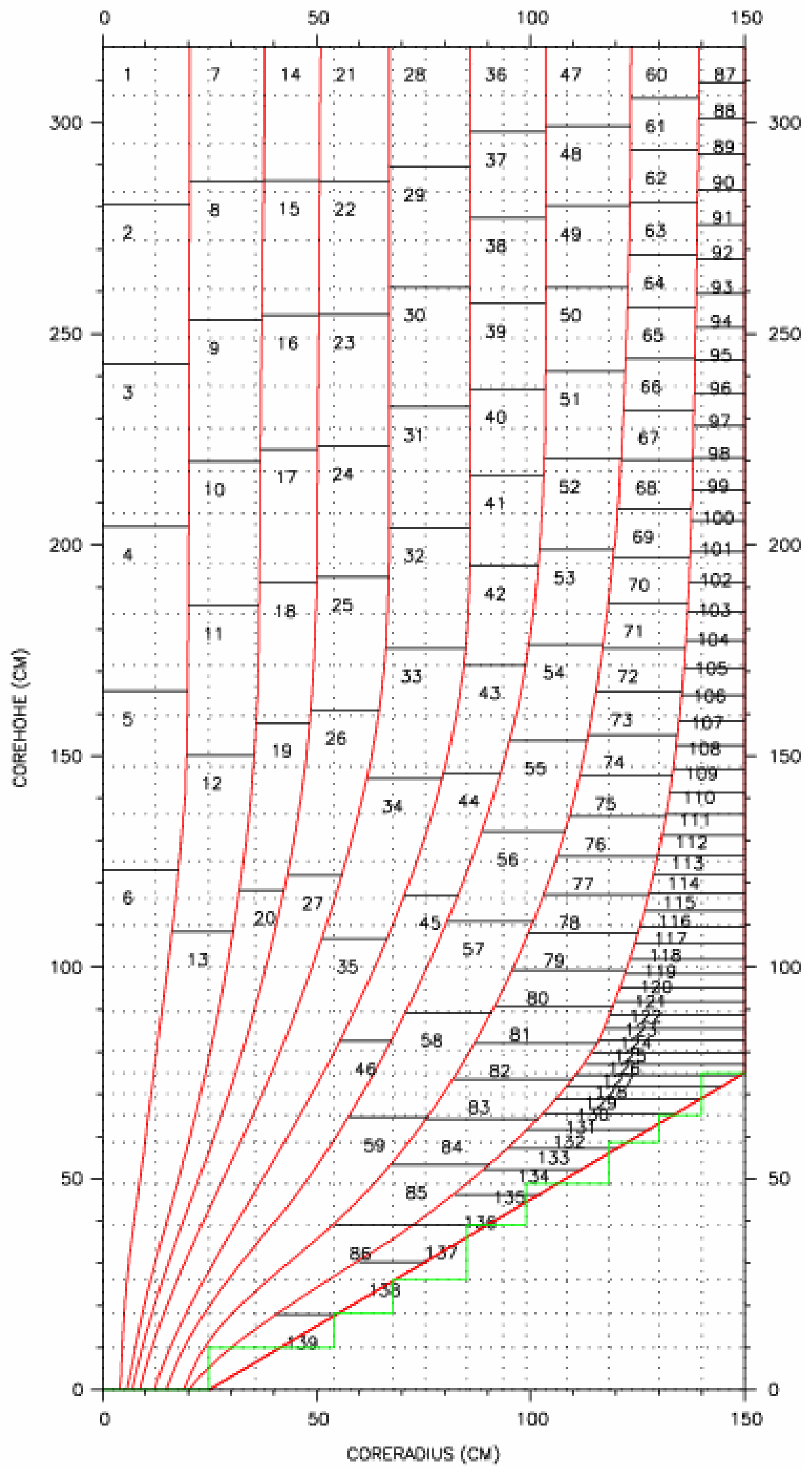

Figure 8: Core model (3D-model) regarding pebble flow lines and (139) burn-up regions

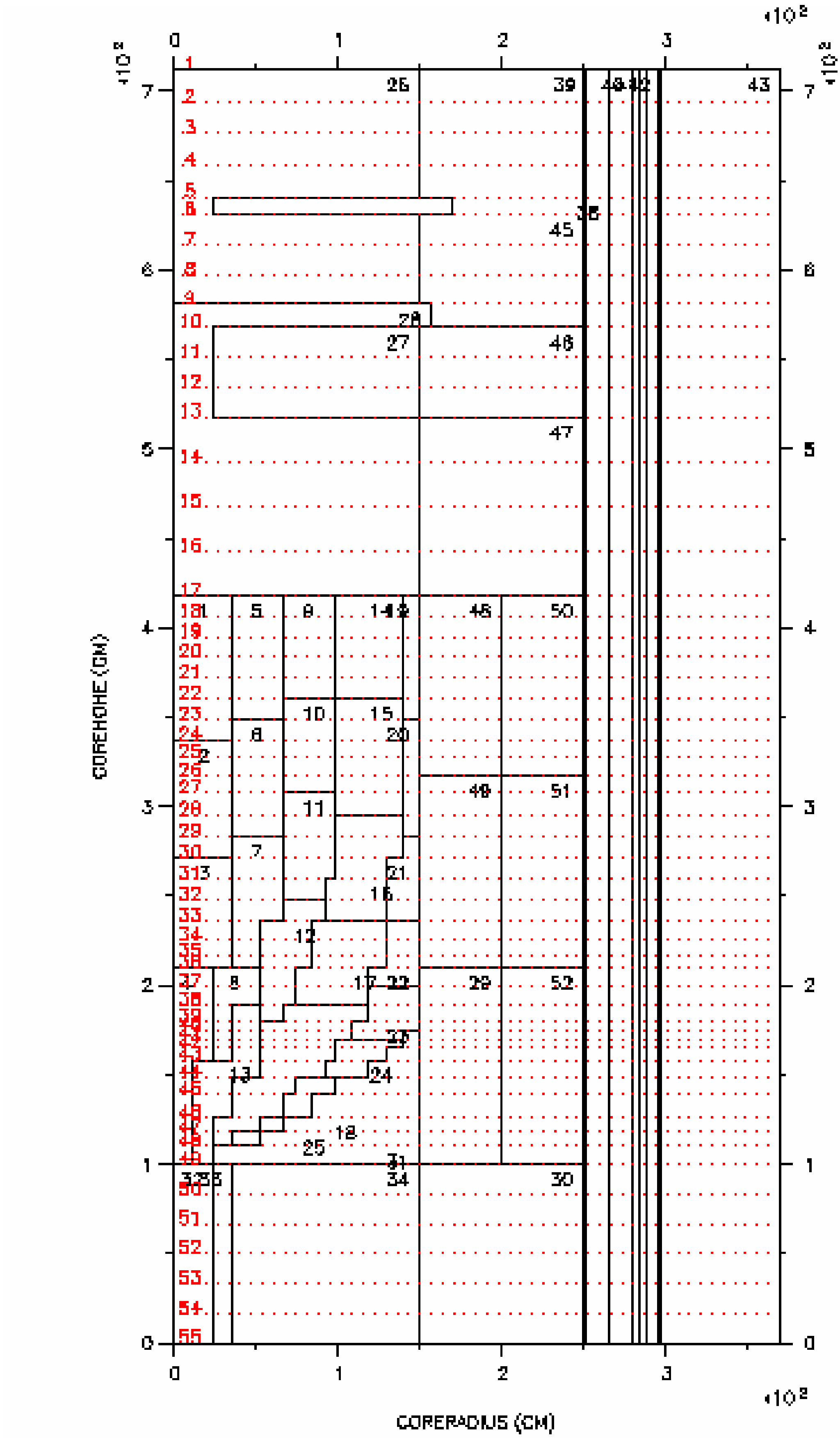

Figure 9: Subdivision of AVR core for neutronics and thermal hydraulics calculations

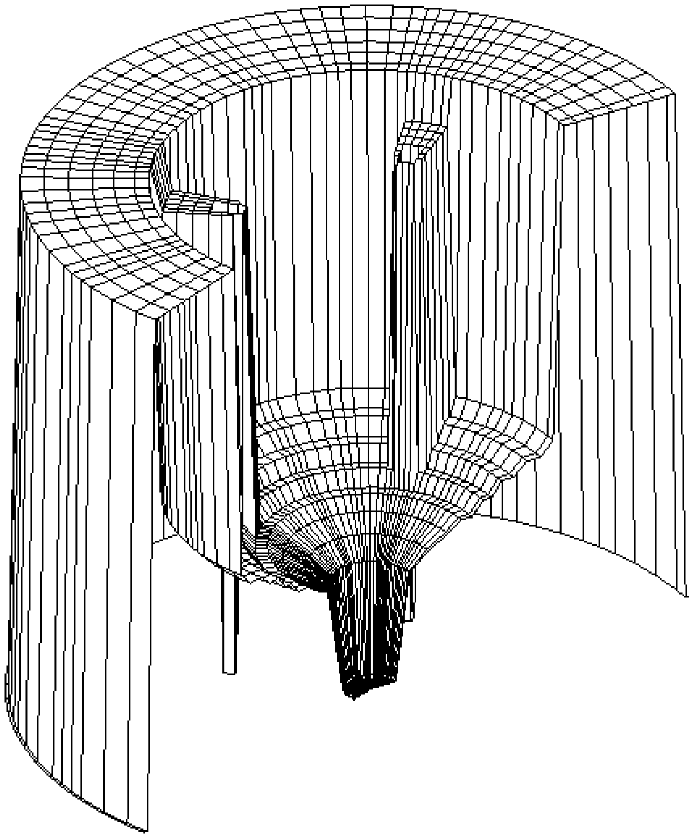

Figure 10: 3D grid for AVR (as realised in HTR-2000 system [3])

The compositions of the different core zones were calculated by H. Werner, FZJ with the HTR-2000 system [.3]. A typical 3D mesh grid for the solution of the neutron diffusion equation is shown in Figure 10. The azimuthal grid is shown in Figure 11.

The composition of the reflector zones is given in Tab.3b. For all compositions (including core materials) the number densities are given for 77 different nuclides (corresponding to AVR-2000 model). The nuclide list is shown in Table 3a. the number densities of the fresh fuel of the fuel types 1-9 are given in Tab. 3c. The composition of the core zones are described in detail in Appendix 1. The geometrical position of these core zones can be seen from Fig. 8. The exact coordinates of these zones (2D, 3D) are described in Appendix 1, too.

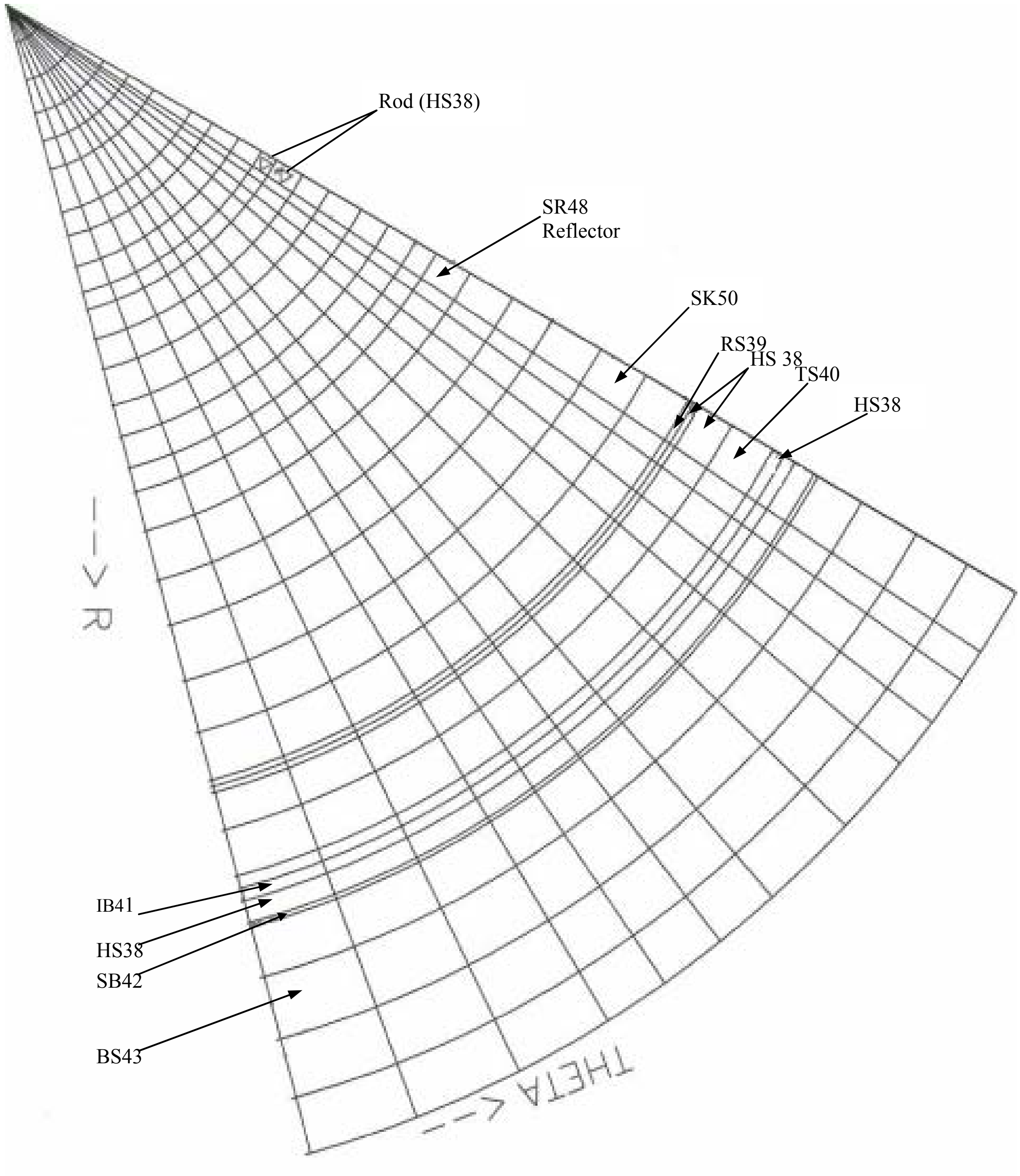

Abbreviations:

HS38	Hohlraum	cavity
RS39	Reaktor-Schalung (Stahl)	barrel (steel)
TS40	Thermischer Schild (Stahl)	thermal shield (steel)
IB41	Innerer Behälter (Stahl)	inner container (steel)
SB42	Schutz-Behälter (Stahl)	protection container (steel)
BS43	Biologischer Schild (mixture 80% Fe)	Biological shield
SK50	Seiten-Reflektor Kohlestein	side reflector carbon
SR48	Seiten-Reflektor Grafit	side reflector graphite

Figure 11: Azimuthal grid for AVR model (45 ° section)

Table 3: List of nuclide names for core and structure material compositions

Table 3a

Nuclides no.	Names of the core and structure materials composition	Nuclides no.	Names of the core and structure materials composition
1	TH-232	40	ND-145
2	PA-233	41	ND-147
3	U-233	42	PM-147
4	U-234	43	PM148M
5	U-235	44	PM-148
6	U-236	45	PM-149
7	U-237	46	SM-149
8	NP-237	47	SM-150
9	U-238	48	SM-151
10	NP-239	49	SM-152
11	PU-239	50	SM-153
12	PU-240	51	EU-153
13	PU-241	52	EU-154
14	PU-242	53	EU-155
15	AM-243	54	GD-155
16	CM-244	55	GD-157
17	KR-83	56	NSFP-5
18	ZR-93	57	B-10
19	ZR-95	58	B-NAT
20	MO-95	59	C
21	TC-99	60	SI-28
22	RU-103	61	HF-174
23	RH-103	62	HF-176
24	RU-105	63	HF-177
25	RH-105	64	HF-178
26	PD-108	65	HF-179
27	AG-109	66	HF-180
28	CD-113	67	BA-138
29	I-131	68	FE-56
30	XE-131	69	NI-58
31	XE-133	70	S-32
32	CS-133	71	CA-40
33	CS-134	72	CR-52
34	I-135	73	PB-208
35	XE-135	74	V-51
36	CS-135	75	CU-63
37	CS-137	76	TI-48
38	PR-143	77	MN-55
39	ND-143		

Table 3b: Composition of fresh fuel elements of types 1 – 9

Nuclide	FA-type 1	FA-type 2	FA-type 3	FA-type 4	FA-type 5	FA-type 6	FA-type 7	FA-type 8	FA-type 9
	GK	GO	GLE-1	1/GFB-2	GO(THTR)	GFB-3	GFB-4/5	GLE-3	GLE-4
TH-232	1,29790E-02	1,29790E-02	1,28230E-02	1,28750E-02	0,00000E+00	2,59360E-02	2,64760E-02	0,00000E+00	0,00000E+00
U-234	2,75720E-05	2,75720E-05	2,75720E-05	2,75720E-05	2,41900E-05	2,75720E-05	2,75720E-05	5,39850E-05	6,63710E-05
U-235	2,56260E-03	2,56260E-03	2,56260E-03	2,56260E-03	3,58760E-03	2,56510E-03	2,46010E-03	2,56260E-03	2,56260E-03
U-238	1,90450E-04	1,90450E-04	1,90450E-04	2,11080E-04	4,63050E-02	1,90640E-04	1,82830E-04	2,27720E-02	1,26520E-02
C	9,45430E+00	9,46130E+00	9,77990E+00	9,76640E+00	9,38000E+00	9,49070E+00	9,71210E+00	9,65850E+00	9,72260E+00
SI-28	3,39940E-02	3,45190E-02	0,00000E+00	0,00000E+00	0,00000E+00	0,00000E+00	0,00000E+00	5,63350E-02	3,38030E-02

Explanation of abbreviations :

FA	Fuel assembly
GK	FA with carbidic (U, Th) C_2 mixed particles
GO	FA with oxidic (U, Th) O_2 mixed particles
GLE	FA with low enriched UO_2 particles
GFB	FA with separated UO_2 (feed) and ThO_2 (breed) particles
GO-THTR	FA with oxidic (U, Th) O_2 mixed particles from the THTR FA production

Table 3c: Composition of material zones 26 – 52

	1	3	5	9	11	20	57	59	60	67	68	69	70	71	72	73
Nr.	TH-232	U-233	U-235	U-238	PU-239	MO-95	B-10	C	SI-28	BA-138	FE-56	NI-58	S-32	CA-40	CR-52	PB-208
26								5.4921E-02								
27								5.8552E-02								
28																
29								8.4247E-02								
30								7.4218E-02								
31								7.0599E-02								
32	3.77E-05	5.00E-07	3.3177E-06	5.4918E-05	2.7055E-07			5.2767E-02								
33							5.97E-02	1.4935E-02								
34								5.8462E-02								
35								8.4247E-02								
36								8.4247E-02								
37								8.4247E-02								
38																
39								1.0029E-03			8.4984E-02					
40								7.9230E-04			8.4937E-02	7.2953E-06	7.4207E-05			
41						3.4717E-04		9.9038E-04	9.6470E-04		8.1111E-02				1.6472E-03	
42								7.9230E-04			8.4937E-02	7.2953E-06	7.4207E-05			
43								9.0517E-04	2.2324E-03	1.2029E-03	1.5951E-02		1.5691E-03	3.36E-03		
44								1.0000E-06								3.2847E-02
45								7.4218E-02								
46								8.4247E-02								
47								8.4247E-02								
48								8.4247E-02								
49								8.4247E-02								
50								7.4218E-02								
51								7.4218E-02								
52								7.4218E-02								

Various fuel types were used and tested during operation of AVR. A description of the fuel, CP diameter, enrichment of U-235 and the Th-232 mass is listed in **Table 4**.

Table 4: Description of fuel types in AVR

Type of fuel			GK	GO	GLE-1		1/ GFB-2		
Number of CP types			1	1	2		2		
Protactinium class			2	2	1		3		
Fuel Enrichment CP diameterr		 % µm	$(U/Th)C_2$ 93 400	$(U/Th)O_2$ 93 400	UO_2 15 600	UO_2 U_{nat} 600	UO_2 93 200	ThO_2 - 600	
Mass	U-235	g	1	1	1.32	0.08	1		
	Th-232	g	5	5	-	-	-	10	
	U-ges	g	1.075	1.075	20		1.075		

Type of fuel			GO(THTR)	GFB-3		GFB-4/5		GLE-3	GLE-4
Number of CP types			1	2		2		1	1
Protactinium class			3	2		2		1	1
Fuel Enrichment CP diameterr		 % µm	$(U/Th)O_2$ 93 400	UO_2 93 198	ThO_2 - 500	UC_2 93 198	ThO_2 - 500	UO_2 10 500	UO_2 16.7 500
Mass	U-235	g	0.96	1	-	1	-	1	1
	Th-232	g	10.2	-	5	-	5	-	-
	U-ges	g	1.033	1.075		1.075		10	16.7

The detailed description of the feed and breed particles is given in Table 5. Since some of the descriptions are in German, a glossary is added to understand the descriptions in this table.

Table 5: Fuel type and CP specification of AVR fuel

```
BE-TYP :  GFB-3/4   TYP NR.1   , BRENNSTOFF  UC2  (TH)O2

      feed particle data :

      COATED PARTICLE DATA :

        SM-DICHTE IM KERNEL(G/CCM) =   10.30000
        ANREICHERUNG               =    0.93000
        KERNELRADIUS  (CM)         =    0.00990

       COATING-SCHICHTEN :

        BUFFER:         DICKE (CM) =    0.01000     DICHTE (G/CCM) = 1.20000
        1.PYC-SCHICHT:  DICKE (CM) =    0.00430     DICHTE (G/CCM) = 1.90000
        SIC-SCHICHT:    DICKE (CM) =    0.00300     DICHTE (G/CCM) = 3.20000
        2.PYC-SCHICHT:  DICKE (CM) =    0.00430     DICHTE (G/CCM) = 1.90000

        number of  PARTICLES  =     28306

         breed particle data :

      COATED PARTICLE DATEN :

        SM-DICHTE IM KERNEL(G/CCM) =    8.00000
        ANREICHERUNG               =    0.00000
        KERNELRADIUS  (CM)         =    0.02630

       COATING-SCHICHTEN :

        BUFFER:         DICKE (CM) =    0.00950     DICHTE (G/CCM) = 1.20000
        1.PYC-SCHICHT:  DICKE (CM) =    0.00850     DICHTE (G/CCM) = 1.90000
        SIC-SCHICHT:    DICKE (CM) =    0.00000     DICHTE (G/CCM) = 0.00000
        2.PYC-SCHICHT:  DICKE (CM) =    0.00000     DICHTE (G/CCM) = 1.90000

        number of PARTICLES  =      9333

        FUELLFAKTOR   =    0.0126

  ATOME PRO BRENNELEMENT:

         U235    0.25626E+22
         U238    0.19045E+21
        TH232    0.12979E+23
         O16     0.25957E+23
        SI28     0.33994E+23
         C12     0.94543E+25

  DICHTE DER C-MATRIX(G/CCM) =  1.7300  DICHTE DER C-SCHALE(G/CCM) = 1.7300
  RADIUS BRENNSTOFF-ZONE   (CM) =  2.50
  RADIUS DER KUGEL         (CM) =  3.00
```

Table 5 (Continued)

```
BE-TYP :  GFB-5    TYP NR. 2   , BRENNSTOFF  UCO  (TH)O2


 FUER DIE BRENNSTOFFPARTIKEL GILT :

     COATED PARTICLE DATEN :

       SM-DICHTE IM KERNEL(G/CCM) =   10.30000
       ANREICHERUNG               =    0.93000
       KERNELRADIUS  (CM)         =    0.00990

      COATING-SCHICHTEN :

       BUFFER:         DICKE (CM) =    0.01000     DICHTE (G/CCM) = 1.20000
       1.PYC-SCHICHT:  DICKE (CM) =    0.00430     DICHTE (G/CCM) = 1.90000
       SIC-SCHICHT:    DICKE (CM) =    0.00300     DICHTE (G/CCM) = 3.20000
       2.PYC-SCHICHT:  DICKE (CM) =    0.00430     DICHTE (G/CCM) = 1.90000

       ANZAHL DER PARTIKEL  =     28743


 FUER DIE BRUTSTOFFPARTIKEL GILT :

     COATED PARTICLE DATEN :

       SM-DICHTE IM KERNEL(G/CCM) =    9.50000
       ANREICHERUNG               =    0.00000
       KERNELRADIUS  (CM)         =    0.02500

      COATING-SCHICHTEN :

       BUFFER:         DICKE (CM) =    0.00950     DICHTE (G/CCM) = 1.20000
       1.PYC-SCHICHT:  DICKE (CM) =    0.00850     DICHTE (G/CCM) = 1.90000
       SIC-SCHICHT:    DICKE (CM) =    0.00000     DICHTE (G/CCM) = 0.00000
       2.PYC-SCHICHT:  DICKE (CM) =    0.00000     DICHTE (G/CCM) = 1.90000

       ANZAHL DER PARTIKEL  =      9151

       FUELLFAKTOR   =    0.0109


 ATOME PRO BRENNELEMENT:

        U235    0.25626E+22
        U238    0.19045E+21
       TH232    0.12979E+23
        O16     0.28710E+23
       SI28     0.34519E+23
        C12     0.94613E+25


 DICHTE DER C-MATRIX(G/CCM)    =  1.7300DICHTE DER C-SCHALE(G/CCM)   = 1.7300
 RADIUS BRENNSTOFF-ZONE   (CM) =  2.50
 RADIUS DER KUGEL         (CM) =  3.00
```

Table 5 (continued)

```
BE-TYP :  GK       TYP NR. 3   , BRENNSTOFF (U/TH)C2

      COATED PARTICLE DATEN :

        SM-DICHTE IM KERNEL(G/CCM) =    8.32000
        ANREICHERUNG               =    0.93000
        KERNELRADIUS  (CM)         =    0.02000

       COATING-SCHICHTEN :

        BUFFER:         DICKE (CM) =    0.00520     DICHTE (G/CCM) = 1.20000
        1.PYC-SCHICHT:  DICKE (CM) =    0.01200     DICHTE (G/CCM) = 2.02000
        SIC-SCHICHT:    DICKE (CM) =    0.00000     DICHTE (G/CCM) = 0.00000
        2.PYC-SCHICHT:  DICKE (CM) =    0.00000     DICHTE (G/CCM) = 2.02000

        ANZAHL DER PARTIKEL  =     23801

        FUELLFAKTOR   =    0.0122

  ATOME PRO BRENNELEMENT:

         U235    0.25626E+22
         U238    0.19045E+21
        TH232    0.12823E+23
         O16     0.00000E+00
        SI28     0.00000E+00
         C12     0.97799E+25

  DICHTE DER C-MATRIX(G/CCM)   =  1.7300 DICHTE DER C-SCHALE(G/CCM) = 1.7300
  RADIUS BRENNSTOFF-ZONE  (CM) =  2.50 RADIUS DER KUGEL        (CM) =  3.00

 BE-TYP :  GO       TYP NR. 4   , BRENNSTOFF (U/TH)O2

      COATED PARTICLE DATEN :

        SM-DICHTE IM KERNEL(G/CCM) =    9.86000
        ANREICHERUNG               =    0.92300
        KERNELRADIUS  (CM)         =    0.02000

       COATING-SCHICHTEN :

        BUFFER:         DICKE (CM) =    0.00770     DICHTE (G/CCM) = 1.20000
        1.PYC-SCHICHT:  DICKE (CM) =    0.01080     DICHTE (G/CCM) = 1.84000
        SIC-SCHICHT:    DICKE (CM) =    0.00000     DICHTE (G/CCM) = 0.00000
        2.PYC-SCHICHT:  DICKE (CM) =    0.00820     DICHTE (G/CCM) = 1.84000

        ANZAHL DER PARTIKEL  =     20807 FUELLFAKTOR    =    0.0107

 ATOME PRO BRENNELEMENT:

         U235    0.25626E+22
         U238    0.21108E+21
        TH232    0.12875E+23
         O16     0.31297E+23
        SI28     0.00000E+00
         C12     0.97664E+25
DICHTE DER C-MATRIX(G/CCM)   =  1.7300  DICHTE DER C-SCHALE(G/CCM) = 1.7300
  RADIUS BRENNSTOFF-ZONE  (CM) =  2.50 RADIUS DER KUGEL        (CM) =  3.00
```

Table 5: (continued)

```
BE-TYP :  GLE 1    TYP NR. 5   , BRENNSTOFF UO2


 FUER DIE BRENNSTOFFPARTIKEL GILT :

     COATED PARTICLE DATEN :

       SM-DICHTE IM KERNEL(G/CCM) =   10.39000
       ANREICHERUNG               =    0.14940
       KERNELRADIUS  (CM)         =    0.03070

      COATING-SCHICHTEN :

       BUFFER:         DICKE (CM) =    0.00940     DICHTE (G/CCM) = 1.20000
       1.PYC-SCHICHT:  DICKE (CM) =    0.00800     DICHTE (G/CCM) = 1.97000
       SIC-SCHICHT:    DICKE (CM) =    0.00000     DICHTE (G/CCM) = 0.00000
       2.PYC-SCHICHT:  DICKE (CM) =    0.00000     DICHTE (G/CCM) = 1.97000

       ANZAHL DER PARTIKEL  =      7979


 FUER DIE BRUTSTOFFPARTIKEL GILT :

     COATED PARTICLE DATEN :

       SM-DICHTE IM KERNEL(G/CCM) =   10.60000
       ANREICHERUNG               =    0.00710
       KERNELRADIUS  (CM)         =    0.03090

      COATING-SCHICHTEN :

       BUFFER:         DICKE (CM) =    0.00940     DICHTE (G/CCM) = 1.20000
       1.PYC-SCHICHT:  DICKE (CM) =    0.00800     DICHTE (G/CCM) = 1.97000
       SIC-SCHICHT:    DICKE (CM) =    0.00000     DICHTE (G/CCM) = 0.00000
       2.PYC-SCHICHT:  DICKE (CM) =    0.00000     DICHTE (G/CCM) = 1.97000

       ANZAHL DER PARTIKEL  =      9391

       FUELLFAKTOR   =    0.0325


 ATOME PRO BRENNELEMENT:

        U235    0.35876E+22
        U238    0.46305E+23
       TH232    0.00000E+00
        O16     0.99786E+23
       SI28     0.00000E+00
        C12     0.93800E+25


 DICHTE DER C-MATRIX(G/CCM)   =  1.7300 DICHTE DER C-SCHALE(G/CCM) = 1.7300
 RADIUS BRENNSTOFF-ZONE   (CM) =  2.50
 RADIUS DER KUGEL         (CM) =  3.00
```

Table 5 (continued)

```
BE-TYP :  GFB-1/2  TYP NR. 6   ,  BRENNSTOFF UO2 / THO2

  FUER DIE BRENNSTOFFPARTIKEL GILT :

      COATED PARTICLE DATEN :

        SM-DICHTE IM KERNEL(G/CCM) =   10.77000
        ANREICHERUNG               =    0.93000
        KERNELRADIUS  (CM)         =    0.01040

       COATING-SCHICHTEN :

        BUFFER:         DICKE (CM) =    0.00890     DICHTE (G/CCM) = 0.86000
        1.PYC-SCHICHT:  DICKE (CM) =    0.00810     DICHTE (G/CCM) = 1.93000
        SIC-SCHICHT:    DICKE (CM) =    0.00000     DICHTE (G/CCM) = 0.00000
        2.PYC-SCHICHT:  DICKE (CM) =    0.00000     DICHTE (G/CCM) = 1.93000

        ANZAHL DER PARTIKEL  =     24095


  FUER DIE BRUTSTOFFPARTIKEL GILT :

      COATED PARTICLE DATEN :

        SM-DICHTE IM KERNEL(G/CCM) =    9.94000
        ANREICHERUNG               =    0.00000
        KERNELRADIUS  (CM)         =    0.03000

       COATING-SCHICHTEN :

        BUFFER:         DICKE (CM) =    0.01040     DICHTE (G/CCM) = 0.93000
        1.PYC-SCHICHT:  DICKE (CM) =    0.00780     DICHTE (G/CCM) = 1.91000
        SIC-SCHICHT:    DICKE (CM) =    0.00000     DICHTE (G/CCM) = 0.00000
        2.PYC-SCHICHT:  DICKE (CM) =    0.00000     DICHTE (G/CCM) = 1.91000

        ANZAHL DER PARTIKEL  =     10114

        FUELLFAKTOR   =    0.0192


  ATOME PRO BRENNELEMENT:

         U235    0.25651E+22
         U238    0.19064E+21
        TH232    0.25936E+23
         O16     0.57384E+23
        SI28     0.00000E+00
         C12     0.94907E+25


  DICHTE DER C-MATRIX(G/CCM) =  1.7300 DICHTE DER C-SCHALE(G/CCM)  = 1.7300
  RADIUS BRENNSTOFF-ZONE  (CM) =  2.50
  RADIUS DER KUGEL        (CM) =  3.00
```

Table 5 (continued)

```
BE-TYP :  GO(THTR) TYP NR. 7   ,  BRENNSTOFF (U/TH)O2

      COATED PARTICLE DATEN :

        SM-DICHTE IM KERNEL(G/CCM) =   10.02000
        ANREICHERUNG               =    0.93000
        KERNELRADIUS  (CM)         =    0.02000

       COATING-SCHICHTEN :

        BUFFER:         DICKE (CM) =    0.00850     DICHTE (G/CCM) = 1.20000
        1.PYC-SCHICHT:  DICKE (CM) =    0.00970     DICHTE (G/CCM) = 1.85000
        SIC-SCHICHT:    DICKE (CM) =    0.00000     DICHTE (G/CCM) = 0.00000
        2.PYC-SCHICHT:  DICKE (CM) =    0.00730     DICHTE (G/CCM) = 1.85000

        ANZAHL DER PARTIKEL  =     38060 FUELLFAKTOR    =    0.0195

ATOME PRO BRENNELEMENT:

         U235    0.24601E+22
         U238    0.18283E+21
        TH232    0.26476E+23
         O16     0.58238E+23
        SI28     0.00000E+00
         C12     0.97121E+25

  DICHTE DER C-MATRIX(G/CCM)   =  1.7300 DICHTE DER C-SCHALE(G/CCM) = 1.7300
  RADIUS BRENNSTOFF-ZONE  (CM) =  2.50 RADIUS DER KUGEL        (CM) =  3.00

 BE-TYP :  LEU 10 (GLE3),  TYP NR. 8  ,  BRENNSTOFF UO2

      COATED PARTICLE DATEN :

        SM-DICHTE IM KERNEL(G/CCM) =   10.40000
        ANREICHERUNG               =    0.10000
        KERNELRADIUS  (CM)         =    0.02500

       COATING-SCHICHTEN :

        BUFFER:         DICKE (CM) =    0.00900     DICHTE (G/CCM) = 1.20000
        1.PYC-SCHICHT:  DICKE (CM) =    0.00430     DICHTE (G/CCM) = 1.90000
        SIC-SCHICHT:    DICKE (CM) =    0.00350     DICHTE (G/CCM) = 3.18000
        2.PYC-SCHICHT:  DICKE (CM) =    0.00410     DICHTE (G/CCM) = 1.90000

        ANZAHL DER PARTIKEL  =     16669 FUELLFAKTOR    =    0.0167

  ATOME PRO BRENNELEMENT:

         U235    0.25626E+22
         U238    0.22772E+23
        TH232    0.00000E+00
         O16     0.50670E+23
        SI28     0.56335E+23
         C12     0.96585E+25

  DICHTE DER C-MATRIX(G/CCM) =  1.7300  DICHTE DER C-SCHALE(G/CCM)  = 1.7300
  RADIUS BRENNSTOFF-ZONE  (CM) =  2.50 RADIUS DER KUGEL        (CM) =  3.00
```

Table 5: (continued)

```
BE-TYP :  LEU 6 (GLE4),   TYP NR. 9   ,   BRENNSTOFF UO2


      COATED PARTICLE DATEN :

        SM-DICHTE IM KERNEL(G/CCM) =    10.40000
        ANREICHERUNG               =     0.16666
        KERNELRADIUS  (CM)         =     0.02500

       COATING-SCHICHTEN :

        BUFFER:         DICKE (CM) =     0.00900     DICHTE (G/CCM) = 1.20000
        1.PYC-SCHICHT:  DICKE (CM) =     0.00430     DICHTE (G/CCM) = 1.90000
        SIC-SCHICHT:    DICKE (CM) =     0.00350     DICHTE (G/CCM) = 3.18000
        2.PYC-SCHICHT:  DICKE (CM) =     0.00410     DICHTE (G/CCM) = 1.90000

        ANZAHL DER PARTIKEL  =     10002 FUELLFAKTOR    =    0.0100

  ATOME PRO BRENNELEMENT:

         U235    0.25626E+22
         U238    0.12652E+23
        TH232    0.00000E+00
         O16     0.30429E+23
        SI28     0.33803E+23
         C12     0.97226E+25


  DICHTE DER C-MATRIX(G/CCM) =  1.7300 DICHTE DER C-SCHALE(G/CCM)  =  1.7300
  RADIUS BRENNSTOFF-ZONE  (CM) =  2.50 RADIUS DER KUGEL        (CM) =  3.00
```

Glossary

Dichte	density	Daten	data
Anreicherung	enrichment	Kernel radius	particle radius
Schicht/en	layer/s	Partikel	particle
Anzahl	number	Fuellfaktor	filling factor
Brennstoff	fuel	pro	per
Brutstoff	breed	Dicke	thickness
Brennelement	fuel element		
Schale	shell		
Kugel	sphere		
Brutpartikel	breed particle		

The data of Table 5 must be regarded together with the zonewise content of fuel element types and fuel element classes with corresponding nuclide composition due to different enrichment and burnup. The list of zonewise fuel types and classes and the corresponding number densities for several reactor states during the time period March – October will be given on a separate data file. A 3D grid with r-theta-z meshes and zone numbers/mesh is specified in the data file "gitter0-1" which is attached to the data base directory for this benchmark From this grid the corresponding geometrical model for the neutronics and thermal hydraulics can be derived for the benchmark calculation. The grid is given for a discretisation chosen for the HTR-2000 system. Other (finer or coarser) grids can be derived from this grid. A further information of the zone subdivision of the core model can be seen from file "avr0-1.prepro".

5 AVR operational data before and during benchmark experiments

The experiments which are the basis for the benchmarks were performed in March and October 1988. Therefore, it was necessary to prepare corresponding core data by simulations of many recycling steps with the program system HTR-2000 regarding the operational data for this period an a substantial time before. These work was performed by H. Werner of FZJ. The data itself (number densities for fuel element classes and zones) are given in special data files prepared for different core states. The structure of these data are described in the header of the files. The main core data – inlet temperature, outlet temperature and power history are given in Figs. 12, 13 and 14 for the year 1988 (until end of October). The begin and end of the interesting experiments are marked in these figures by arrows. The detailed operational data during the corresponding experiments are described together with the description of the experiments.

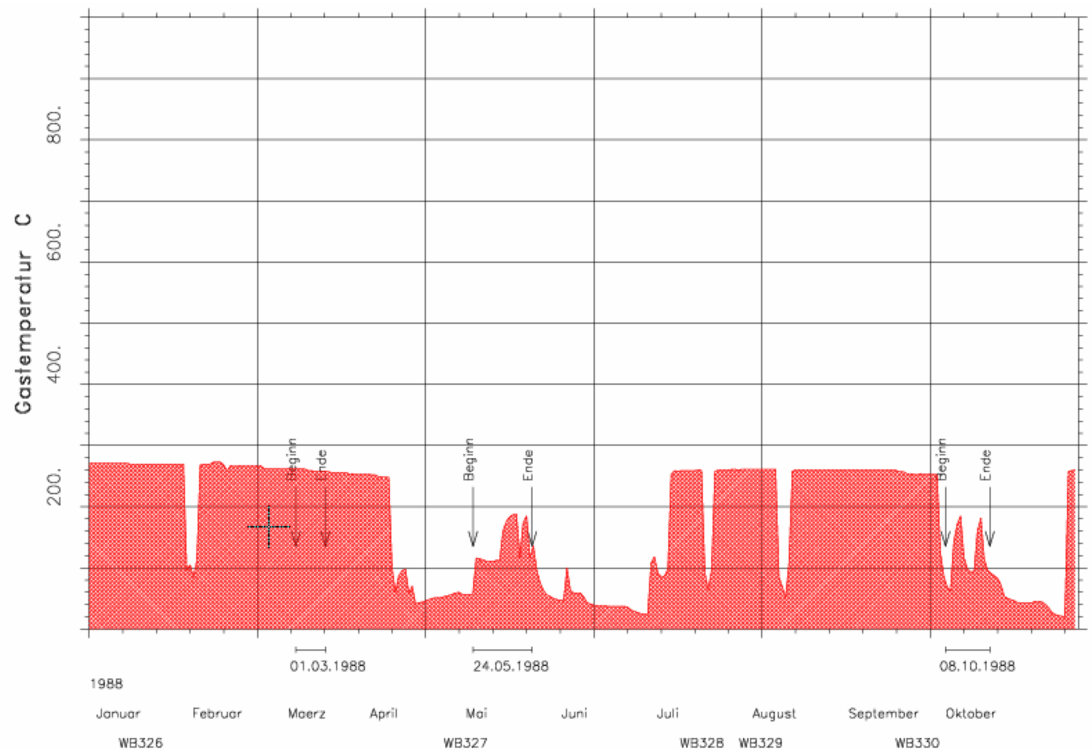

Figure 12: Helium inlet temperature for January to end of October 1988 in AVR

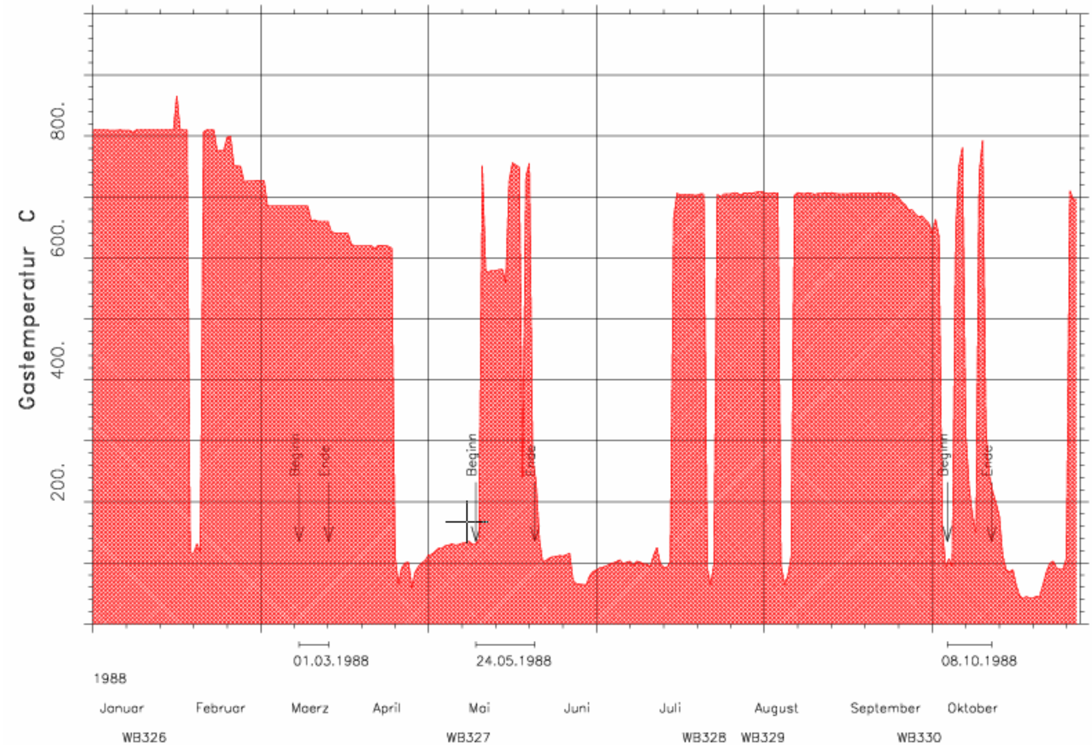

Figure 13: Helium outlet temperatures for January to End of October 1988 in AVR

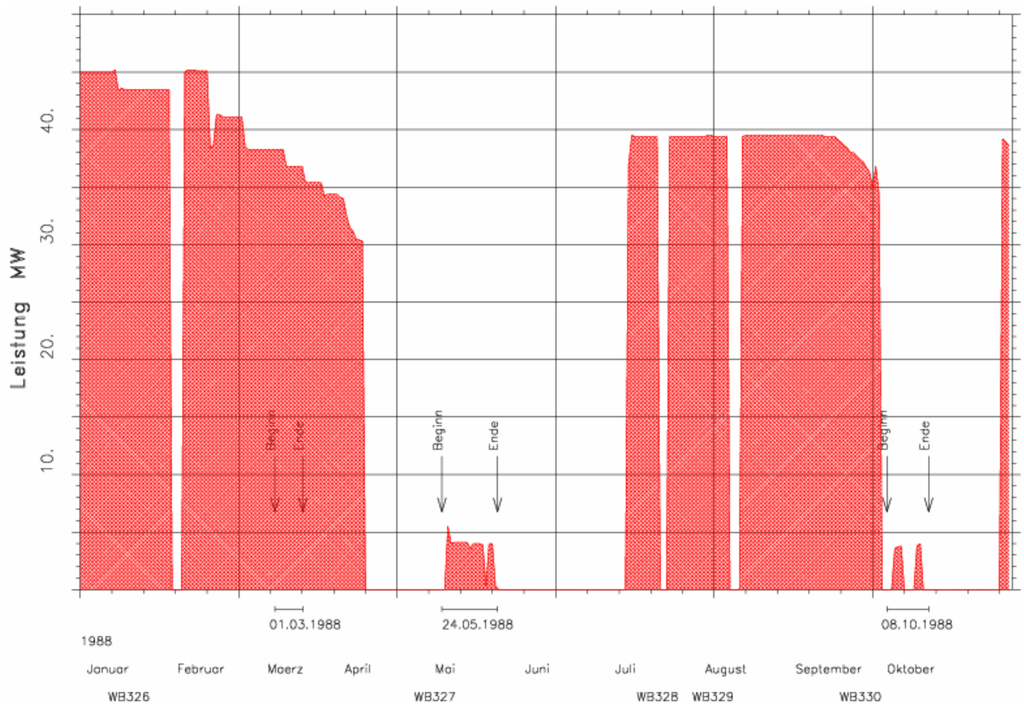

Figure 14: Power history for January to end of October 1988 in AVR

6 Description of benchmark experiments

6.1 Dynamics experiments

In March 1988 dynamics experiments were performed with the core partly filled with LEU fuel. The reactor was operated from January to End of February 1988 with constant full power and 810°C, interrupted by a short shutdown interval from 21st to 25th February 1988. One day before the first experiment the He exit temperature was lowered at full power from 810 to 775 °C to be able to start all following experiments at identical temperature.

Following experiments were performed :

- Reduction of mass flow to 50% and return to 100%
- Insertion of control rods
- Reduction of mass flow to 80% and subsequent Xe-transient

The description of the three experiments is given in Table 6.

The experimental results are described in [**4**]. The main experimental data from [**4**] are given in Table 7 to Table 10 of this report. In Figure 15 to Figure 17 the relative neutron flux and the relative rotation speed of the blower is shown as a function of time. The requested data are the relative change in neutron flux density and corresponding change in reactor power and outlet temperature. The power of the steam generator and the inlet temperature is reported in [**4**] and Table 7 to Table 10 respectively and can be used as boundary conditions during the transients.

Table 6: Chronology of dynamic experiments

Date	time	Experiment	Results in Table
01/03/1988	10:05	Fast reduction of mass flow to 50% with constant control rod positions	7
	10:35	Fast increase of mass flow to 78% with constant control rod positions	8
02/03/1988	14:46	Insertion of all four control rods with constant speed corresponding to 66 mNile starting from full power. The Insertion depth was 117 mm. The mass flow was kept constant	9
03/03/1988	13:38	Fast reduction of blower speed to 79 % of full speed without moving control rods or changing blower speed. The following 48 hours there was no operational action, a Xe transient followed	10
05/03/1988	13:38	End of experiment	

The meanings of the symbols in the tables 7-10 in ref. [**4**] are:

$\phi_n = \frac{\phi_n(t)}{\phi_n(t=0)}$ relative time dependency of neutron flux in %

$n_{Gebl.}$	revolutions/minute of blower
$\Delta P_{Gebl.}$	Pressure drop of fluid over blowers
P_{KG}	Pressure of coolant gas in inner reactor vessel
ϑ_{eG}	Coolant gas temperature at core inlet
ϑ_{aG_M}	Temperature of coolant gas in top reflector (outlet)
ϑ_{aG_R}	Calculated outlet temperature (from inlet temperature, He mass flow and power of steam generator (stationary conditions)
P_{DE}	Power of steam generator (stationary conditions)

Table 7: Experimental results for decrease of rotation speed 100 to 50 % [4]

t/s		ϕ_n/%	^{n}Gebl.	$^{\Delta p}$Gebl.	^{p}KG	$^{\vartheta}$eG	$^{\vartheta}$aG$_M$	$^{\vartheta}$aG$_R$	^{P}DE
			min^{-1}	mbar	bar	°C	°C	°C	MW
0		100,00	4254,0	78,1	9,76	274,0	828,0	775	45,2
12		99,00	3841,0	63,7	9,74	273,5	828,0	775	45,2
24		94,90	3427,9	51,0	9,71	273,0	828,5	775	45,2
36		87,80	3014,9	39,2	9,68	272,0	829,5	775	45,2
48		79,55	2601,9	30,0	9,64	271,0	830,0	775	45,2
60		70,00	2188,8	21,6	9,61	269,5	830,5	775	45,2
62	1)	70,00	2120,0	21,6	9,61	269,5	830,5	775	45,2
62,5		70,00	2120,0	20,2	9,61	269,5	830,5	775	45,2
72		61,00	2120,0	20,2	9,58	269,5	831,0	775	45,2
84		54,00	2119,9	20,2	9,58	269,5	831,0	775	45,2
96		48,80	2119,9	20,2	9,58	268,0	832,0	775	45,2
108		44,90	2119,9	20,2	9,56	268,0	832,0	775	45,2
120		42,10	2119,9	20,2	9,56	266,5	832,5	775	45,2
132		40,40	2119,8	20,2	9,56	266,5	832,5	775	45,2
144		39,55	2119,8	20,2	9,54	266,5	832,5	775	45,2
156		39,40	2119,8	20,2	9,54	266,5	832,5	775	45,2
168		39,90	2119,8	20,2	9,53	266,5	832,5	775	45,2
180		41,10	2119,7	20,2	9,53	264,5	832,0	775	45,2
192		42,40	2119,7	20,2	9,53	264,5	832,0	775	45,2
204		44,30	2119,7	20,2	9,53	264,5	832,0	775	45,2
216		46,20	2119,6	20,2	9,53	264,5	832,0	775	45,2
228		48,00	2119,6	20,2	9,52	264,5	832,0	775	45,2
240		49,80	2119,6	20,2	9,52	264,0	831,0	775	45,2
252		51,00	2119,6	20,2	9,52	264,0	831,0	775	45,2
264		51,80	2119,5	20,2	9,52	264,0	831,0	775	45,2
276		52,30	2119,5	20,2	9,53	264,0	831,0	775	45,2
288		52,40	2119,5	20,2	9,53	264,0	831,0	775	45,2
300		52,20	2119,4	20,2	9,54	263,0	832,0	775	45,2
312		52,00	2119,4	20,2	9,54	263,0	832,0	775	45,2
324		51,55	2119,4	20,2	9,54	263,0	832,0	775	45,2
336		51,10	2119,4	20,2	9,55	263,0	832,0	775	45,2
360		50,40	2119,3	20,2	9,55	263,0	832,0	775	45,2
384		50,10	2119,3	20,2	9,56	263,0	832,0	775	45,2
408		50,00	2119,2	20,2	9,56	263,0	832,0	775	45,2
432		50,10	2119,1	20,2	9,56	263,0	832,0	775	45,2
456		50,30	2119,1	20,2	9,56	262,0	834,5	775	45,2
504		50,70	2119,0	20,2	9,55	262,0	834,5	775	45,2
552		50,70	2118,9	20,2	9,54	262,0	834,5	775	45,2
600		50,70	2118,7	20,2	9,52	260,5	836,0	775	45,2
720		50,70	2118,5	20,2	9,50	259,0	835,5	775	45,2
840		50,70	2118,2	20,2	9,50	257,5	835,0	775	45,2
960		50,70	2117,9	20,2	9,50	256,5	835,0	775	45,2
1080		50,70	2117,6	20,2	9,50	256,0	834,5	775	45,2
1200		50,70	2117,4	20,2	9,50	255,5	834,0	775	45,2
1320		50,70	2117,1	20,2	9,50	255,0	833,5	775	45,2
1440		50,70	2116,8	20,2	9,50	254,5	833,0	794	23,6
1560		50,55	2116,5	20,2	9,50	254,0	832,0	794	23,6
1680		50,40	2116,2	20,2	9,50	253,5	832,0	794	23,6
1782	2)	50,40	2116,0	20,4	9,50	253,0	831,0	794	23,6

1) End of decrease of rotation speed
2) Begin of increase of rotation speed

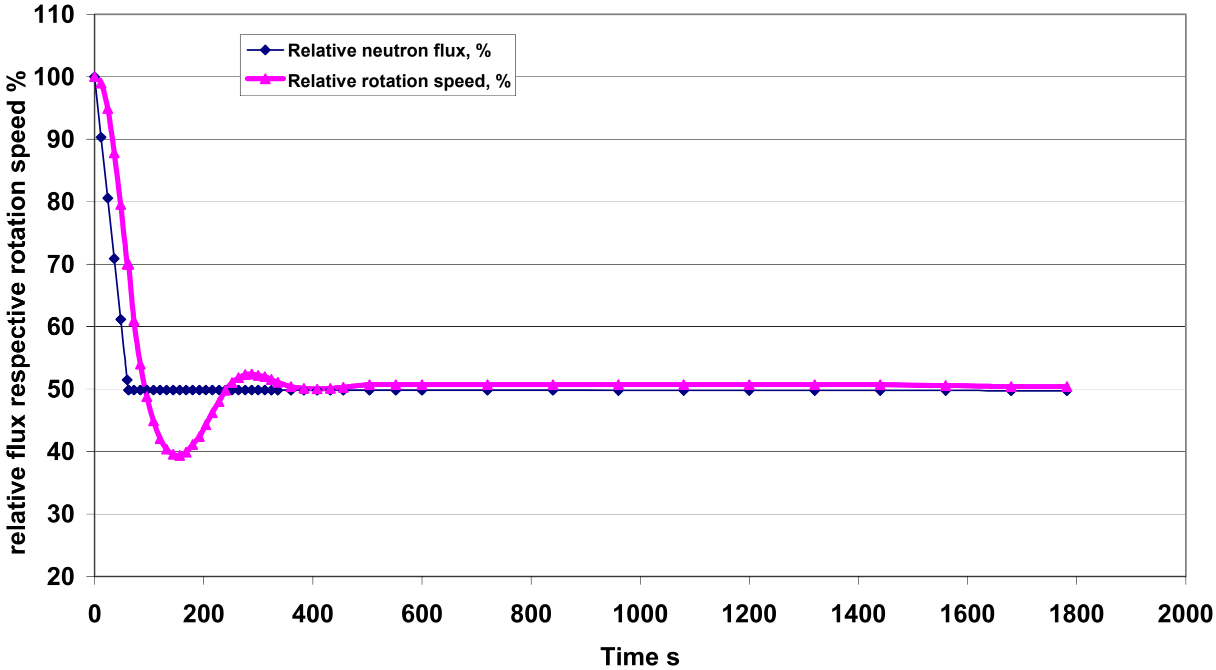

Figure 15: Experimental results for decrease of rotation speed 100 to 50 % [4]

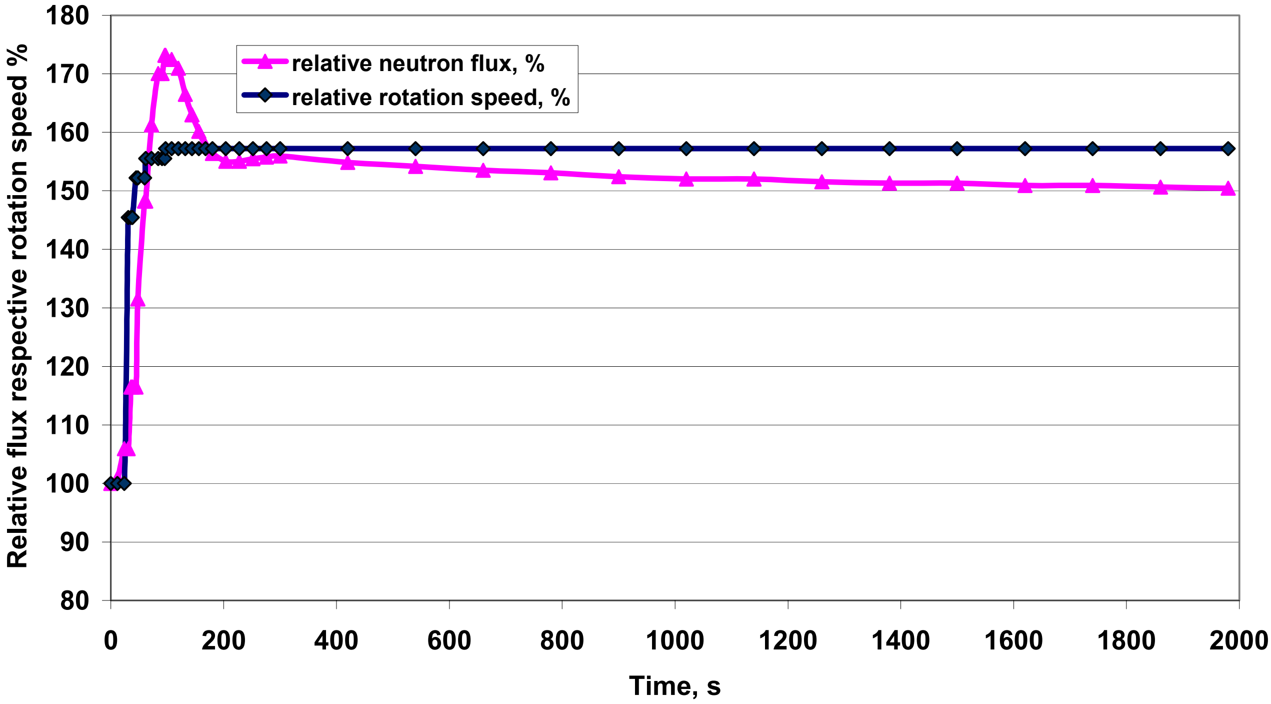

Figure 16: Experimental results for increase of rotation speed 50 to 100 % [4]

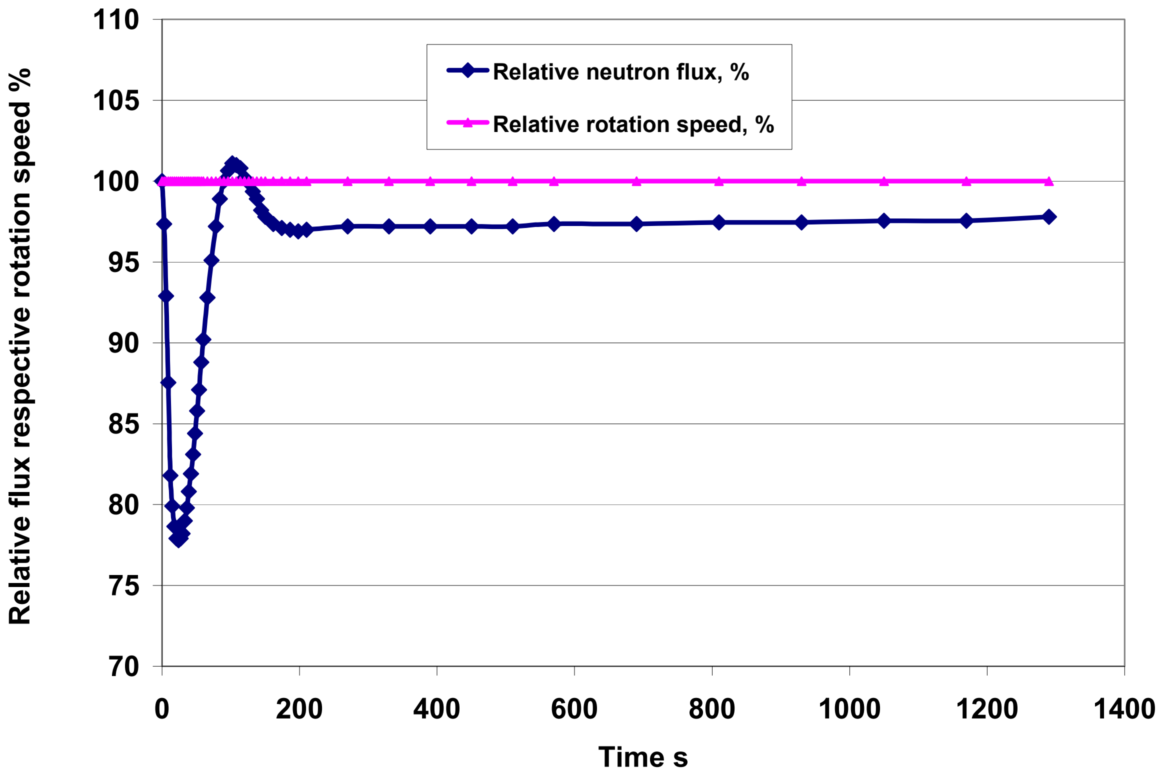

Figure 17: Experimental results for control rod insertion [4]

Table 8: Experimental results for increase of rotation speed 50 to 100 % [4]

t/s		ϕ_n/%	^{n}Gebl.	$^{\Delta p}$Gebl.	^{p}KG	$^{\vartheta}$eG	$^{\vartheta}$aG$_M$	$^{\vartheta}$aG$_R$	^{P}DE
			min^{-1}	mbar	bar	°C	°C	°C	MW
0,0	1)	100,00	2116	20,4	9,50	253,0	831,0		
12,0		100,90	2116	27,4	9,51	253,5	831,5		
24,0		105,95	2116	35,9	9,53	254,0	831,5		
30,8		105,95	3078	41,6	9,53	254,0	831,5		
36,0		116,50	3078	41,6	9,55	254,5	831,5		
38,5		116,50	3078	41,6	9,55	254,5	831,5		
45,0		116,50	3221	45,6	9,55	254,5	831,5		
48,0		131,50	3221	45,6	9,55	255,0	830,0		
60,0		148,25	3221	45,6	9,55	255,0	829,5		
62,1		148,25	3291	47,8	9,55	255,0	829,5		
72,0		161,25	3291	47,8	9,55	255,5	829,0		
84,0		170,05	3291	47,8	9,55	255,5	829,0		
91,1		170,05	3291	47,8	9,55	255,5	829,0		
96,0		173,15	3291	47,8	9,55	255,5	828,0		
97,1	2)	173,15	3327	48,8	9,55	255,5	828,0		
108,0		172,45	3327	48,8	9,57	255,5	828,0		
120,0		170,95	3327	48,8	9,57	256,0	827,5		
132,0		166,50	3327	48,8	9,57	256,0	827,5		
144,0		163,00	3327	48,8	9,57	256,0	827,5		
156,0		160,15	3327	48,8	9,57	256,0	827,5		
168,0		157,70	3327	48,8	9,57	256,0	827,5		
180,0		156,40	3327	48,8	9,57	256,5	827,5		
204,0		155,05	3327	48,8	9,57	256,5	827,5		
228,0		155,05	3327	48,8	9,57	256,5	827,5		
252,0		155,50	3327	48,8	9,57	256,5	825,0		
276,0		155,75	3327	48,8	9,57	256,5	825,0		
300,0		155,95	3327	48,8	9,58	257,5	824,5		
420,0		154,85	3327	48,8	9,58	258,0	823,0		
540,0		154,20	3327	48,8	9,58	259,0	822,0		
660,0		153,50	3327	48,8	9,58	259,5	821,0		
780,0		153,10	3327	48,8	9,58	259,5	820,0		
900,0		152,40	3327	48,8	9,59	259,5	819,0		
1020,0		152,00	3327	48,8	9,59	259,5	818,0		
1140,0		152,00	3327	48,8	9,59	260,5	818,0		
1260,0		151,55	3327	48,8	9,59	260,5	817,0		
1380,0		151,30	3327	48,8	9,59	260,5	816,0		
1500,0		151,30	3327	48,8	9,59	260,0	815,5	766	35,5
1620,0		150,90	3327	48,8	9,59	260,0	815,0	766	35,5
1740,0		150,90	3327	48,8	9,59	260,0	814,5	766	35,5
1860,0		150,65	3327	48,8	9,59	260,0	814,0	766	35,5
1980,0		150,45	3327	48,4	9,60	260,0	813,0	766	35,5

1) End of decrease of rotation speed
2) Begin of increase of rotation speed

Table 9: Experimental results for control rod insertion [4]

t/s		ϕ_n/%	^{n}Gebl.	$^{\Delta p}$Gebl.	^{P}KG	$^{\vartheta}$eG	$^{\vartheta}$aG$_M$	$^{\vartheta}$aG$_R$	^{P}DE
			min^{-1}	mbar	bar	°C	°C	°C	MW
0	1)	100,00	4260	78,2	9,8	273,0	818,0	777	45,2
3		97,35	4260	78,2	9,8	273,0	818,0	777	45,2
6		92,90	4260	78,2	9,8	273,0	818,0	777	45,2
9		87,55	4260	78,2	9,8	273,0	818,0	777	45,2
12	2)	81,80	4260	78,2	9,8	273,0	817,5	777	45,2
15		79,90	4260	78,2	9,8	273,0	817,5	777	45,2
18		78,65	4260	78,2	9,8	273,0	817,5	777	45,2
21		77,90	4260	78,2	9,8	273,0	817,5	777	45,2
24		77,80	4260	78,2	9,8	273,0	817,5	777	45,2
27		77,90	4260	78,2	9,8	273,0	817,5	777	45,2
30		78,20	4260	78,2	9,8	273,0	816,5	777	45,2
33		79,00	4260	78,2	9,8	273,0	816,5	777	45,2
36		79,80	4260	78,2	9,8	273,0	816,5	777	45,2
39		80,80	4260	78,2	9,8	273,0	816,5	777	45,2
42		81,90	4260	78,2	9,8	273,0	816,5	777	45,2
45		83,10	4260	78,2	9,8	273,0	816,5	777	45,2
48		84,40	4260	78,2	9,8	273,0	816,5	777	45,2
51		85,80	4260	78,2	9,8	273,0	816,5	777	45,2
54		87,10	4260	78,2	9,8	273,0	816,5	777	45,2
57		88,80	4260	78,2	9,8	273,0	816,5	777	45,2
60		90,20	4260	78,2	9,8	273,0	813,0	777	45,2
66		92,80	4260	78,2	9,8	273,0	813,0	777	45,2
72		95,10	4260	78,2	9,8	272,5	813,0	777	45,2
78		97,20	4260	78,2	9,8	272,5	813,0	777	45,2
84		98,90	4260	78,2	9,8	272,5	813,0	777	45,2
90		100,00	4260	78,2	9,8	272,5	811,0	777	45,2
96		100,65	4260	78,2	9,8	272,5	811,0	777	45,2
102		101,10	4260	78,2	9,8	272,5	811,0	777	45,2
108		101,00	4260	78,2	9,8	272,5	811,0	777	45,2
114		100,80	4260	78,2	9,8	272,5	811,0	777	45,2
120		100,20	4260	78,2	9,8	272,5	810,0	777	45,2
126		99,90	4260	78,2	9,8	272,5	810,0	777	45,2
132		99,35	4260	78,2	9,8	272,5	810,0	777	45,2
138		98,90	4260	78,2	9,8	272,5	810,0	777	45,2
144		98,20	4260	78,2	9,8	272,5	810,0	777	45,2
150		97,80	4260	78,2	9,8	272,5	810,0	777	45,2
162		97,35	4260	78,2	9,8	272,5	810,0	777	45,2
174		97,10	4260	78,2	9,8	272,5	810,0	777	45,2
186		97,00	4260	78,2	9,8	272,5	809,0	777	45,2
198		96,90	4260	78,2	9,8	272,5	809,0	777	45,2
210		97,00	4260	78,2	9,8	272,0	809,0	777	45,2
270		97,20	4260	78,2	9,8	272,0	808,0	777	45,2
330		97,20	4260	78,2	9,8	272,0	807,0	777	45,2
390		97,20	4260	78,2	9,8	272,0	807,0	777	45,2
450		97,20	4260	78,2	9,8	271,5	806,5	777	45,2
510		97,20	4260	78,2	9,8	271,5	806,5	777	45,2
570		97,35	4260	78,2	9,8	271,5	806,0	777	45,2
690		97,35	4260	78,2	9,8	271,5	806,0	777	45,2
810		97,45	4260	78,2	9,8	270,5	805,5	777	45,2
930		97,45	4260	78,2	9,8	270,5	805,5	777	45,2
1050		97,55	4260	78,2	9,8	270,0	805,0	777	45,2
1170		97,55	4260	78,2	9,8	270,0	805,0	777	45,2
1290		97,80	4260	78,2	9,8	269,0	805,0	766	44,6

1) Begin of inserting of control rod
2) End of inserting of control rod

Table 10: Experimental results for decrease of rotation speed to 80% followed by Xe transient [4]

t		ϕ_n/%	^{n}Gebl.	$^{\Delta p}$Gebl.	^{p}KG	$^{\vartheta}$eG	$^{\vartheta}$aG$_M$	$^{\vartheta}$aG$_R$	^{P}DE
s			min^{-1}	mbar	bar	°C	°C	°C	MW
0		100,00	4258	78,2	9,77	273,0	820,5	775	45,1
12		98,90	4255	64,0	9,75	273,0	821,0	775	45,1
24		94,75	4254	64,0	9,72	272,0	821,5	775	45,1
26	1)	94,75	3359	49,2	9,72	272,0	821,5	775	45,1
36		88,35	3359	49,2	9,71	271,5	822,0	775	45,1
48		82,65	3359	49,2	9,71	271,5	823,0	775	45,1
60		78,55	3359	49,2	9,70	271,0	824,0	775	45,1
72		75,90	3359	49,2	9,70	271,0	824,0	775	45,1
84		74,55	3359	49,2	9,70	271,0	824,0	775	45,1
96		74,20	3359	49,2	9,70	271,0	824,0	775	45,1
108		74,65	3359	49,2	9,70	271,0	824,0	775	45,1
120		75,55	3359	49,2	9,70	270,0	824,5	775	45,1
132		76,65	3359	49,2	9,70	270,0	824,5	775	45,1
144		77,75	3359	49,2	9,70	270,0	824,5	775	45,1
156		78,65	3359	49,2	9,70	270,0	824,5	775	45,1
168		79,45	3359	49,2	9,70	270,0	824,5	775	45,1
180		80,00	3359	49,2	9,70	269,5	824,5	775	45,1
192		80,35	3359	49,2	9,70	269,5	824,5	775	45,1
204		80,35	3359	49,2	9,70	269,5	824,5	775	45,1
228		80,20	3359	49,2	9,70	269,5	824,5	775	45,1
252		80,00	3359	49,2	9,70	269,0	824,5	775	45,1
276		80,00	3359	49,2	9,70	269,0	824,5	775	45,1
300		80,00	3359	49,2	9,70	268,5	826,0	775	45,1
360		80,00	3359	49,2	9,70	268,0	826,0	775	45,1
420		80,20	3359	49,2	9,70	268,0	826,0	775	45,1
480		80,20	3359	49,2	9,70	267,5	826,0	775	45,1
540		80,35	3359	49,2	9,70	267,5	826,0	775	45,1
600		80,35	3359	49,2	9,70	267,0	826,0	775	45,1
900		80,45	3359	49,2	9,70	266,5	826,0	775	45,1
1200		80,65	3359	49,2	9,70	264,5	825,0	775	45,1
1500		80,55	3359	49,2	9,71	264,0	825,0	775	45,1
1800		80,35	3359	49,8	9,72	264,0	823,0	774	36,5
3600		79,20	3359	49,8	9,74	259,5	816,5	762	36,2
7200		77,55	3359	50,0	9,77	259,5	803,5	762	36,2
10800		75,55	3359	50,0	9,77	259,5	792,0	762	36,2
14400		74,45	3359	50,0	9,77	259,0	785,0	762	36,2
18000		74,20	3359	50,0	9,77	257,5	781,5	736	34,8
21600		74,45	3358	50,0	9,77	256,5	782,0	736	34,8
25200		74,65	3357	50,0	9,77	256,5	784,0	736	34,8
28800		75,35	3356	50,0	9,77	256,5	789,0	736	34,8
32400		76,65	3355	50,0	9,77	256,0	795,0	746	35,7
36000		77,90	3355	50,4	9,77	255,5	803,0	746	35,7
39600		78,90	3355	50,4	9,77	265,5	810,5	746	35,7
43200		80,10	3355	50,4	9,77	265,5	818,0	746	35,7
46800		81,10	3355	50,4	9,77	258,0	825,0	776	37,3
50400		82,20	3355	50,4	9,77	258,0	831,0	776	37,3
54000		83,30	3355	50,6	9,77	258,0	838,0	776	37,3
57600		84,10	3355	50,6	9,77	258,5	842,5	776	38,4
61200		84,65	3355	50,6	9,77	259,0	846,5	798	38,4
64800		85,20	3354	50,6	9,77	259,5	849,5	798	38,4
68400		85,55	3354	50,6	9,77	259,5	851,5	798	38,4
72000		85,90	3353	50,6	9,77	259,5	853,5	798	38,4
75600		86,20	3352	50,6	9,77	259,5	855,0	807	38,9
79200		86,45	3352	50,6	9,77	259,5	856,0	807	38,9
82800		86,55	3352	50,6	9,77	259,5	856,5	807	38,9
86400		86,55	3352	50,6	9,77	259,5	857,0	807	38,9
90000		86,45	3352	50,6	9,77	259,5	856,5	809	39,1

Table 10 (continuation)

93600	86,45	3352	50,6	9,77	259,5	856,0	809	39,1
97200	86,35	3352	50,6	9,77	259,0	855,0	809	39,1
100800	86,20	3352	50,6	9,77	259,0	854,5	809	39,1
104400	86,00	3352	50,6	9,77	259,0	853,5	806	39,0
108000	86,00	3352	50,6	9,77	259,0	853,0	806	39,0
111600	85,90	3351	50,6	9,77	258,5	852,0	806	39,0
115200	85,75	3351	50,6	9,77	258,5	851,0	806	39,0
118800	85,55	3350	50,6	9,77	258,5	850,0	806	38,9
122400	85,55	3350	50,6	9,77	258,0	849,5	806	38,9
126000	85,55	3350	50,6	9,77	258,0	849,0	806	38,9
129600	85,35	3350	50,6	9,77	258,0	848,5	806	38,9
133200	85,10	3350	50,6	9,77	258,0	848,0	805	38,8
136800	85,00	3350	50,6	9,77	258,0	847,0	805	38,8
140400	84,90	3350	50,6	9,77	258,0	846,0	805	38,8
144000	84,90	3350	50,6	9,77	258,0	845,5	805	38,8
147600	84,75	3350	50,6	9,77	258,0	845,0	799	38,6
151200	84,75	3350	50,6	9,77	257,5	845,0	799	38,6
154800	84,45	3350	50,6	9,77	258,0	844,5	799	38,6
158400	84,45	3350	50,6	9,77	258,0	843,5	799	38,6
162000	84,45	3350	50,6	9,77	258,0	843,0	793	38,3
165600	84,45	3350	50,6	9,77	258,0	842,5	793	38,3
169200	84,35	3350	50,6	9,77	258,0	842,5	793	38,3
172800	84,35	3350	50,6	9,77	258,0	841,5	793	38,3

1) **End of decrease of rotation speed**

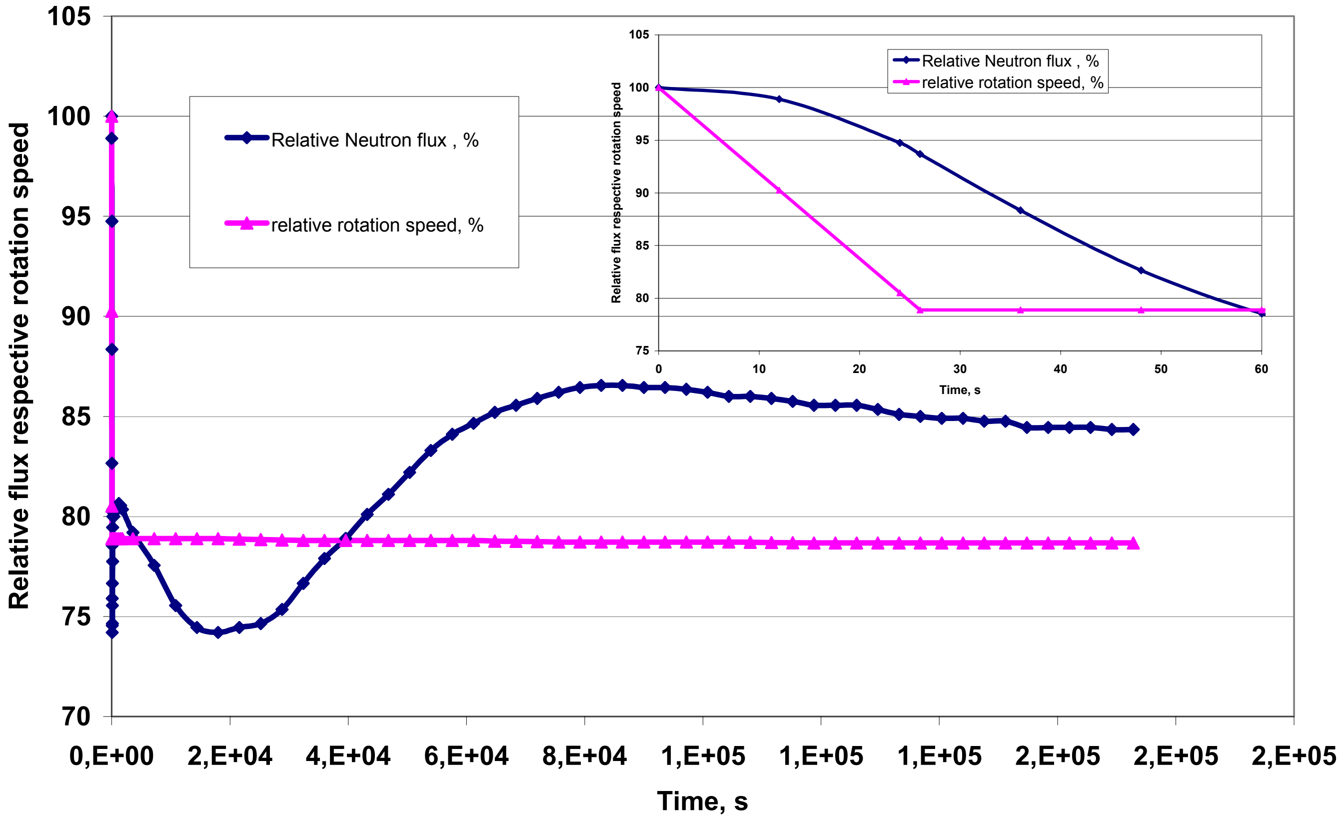

Figure 18: Experimental results for decrease of rotation speed to 80% followed by Xe transient [4]

6.2 Simulation of the LOCA experiment

The experiment was performed by following steps:

- The reactivity was dropped by stop of recirculation of pebbles and the shutdown rods were therefore only slightly inserted.
- Then the reactor was shut down and the cooling gas pressure lowered to 1 bar.
- To get the real starting conditions for LOCA the reactor was operated for some days at low power until the full load temperatures were reached.
- During the actual simulation of the accident the decay heat curve for full load conditions was simulated with fission power, controlled via the shutdown rods.

During the simulation of the accident the temperatures in the core zone and the surrounding metallic internals were recorded for some days. The chronology of the experiment is given in Tab. 11. The experimental data are given in [**4**]. Further informations in [5]. The main input data are the simulated after heat by fission power. The power used in the experiment is given in Figure 19 and in Table 11. A more detailed description of the experiment can be found in **[2**, chapter 5]

Table 11: Chronology of the LOCA simulation experiment

Time after shutdown of blower *)	remaining decay heat **) in kW	Fission Power (after reduction) in kW	Total power (after reduction) in kW
0	331	1062	1393
12 min	156	717	873
30 min	133	569	702
1 h	126	481	607
1,5 h	121	429	550
2 h	116	373	489
3 h	112	329	441
4 h	108	303	411
5 h	105	271	376
7 h	102	240	342
9 h	99	217	316
12 h	97	196	293
15 h	96	168	264
1 d	92	132	224
2 d	87	106	193
3 d	84	84	168
4 d	82	82	164
5 d	80	77	157

*) Time point of fission power reduction
**) Power before shutdown of blower : 4 MW

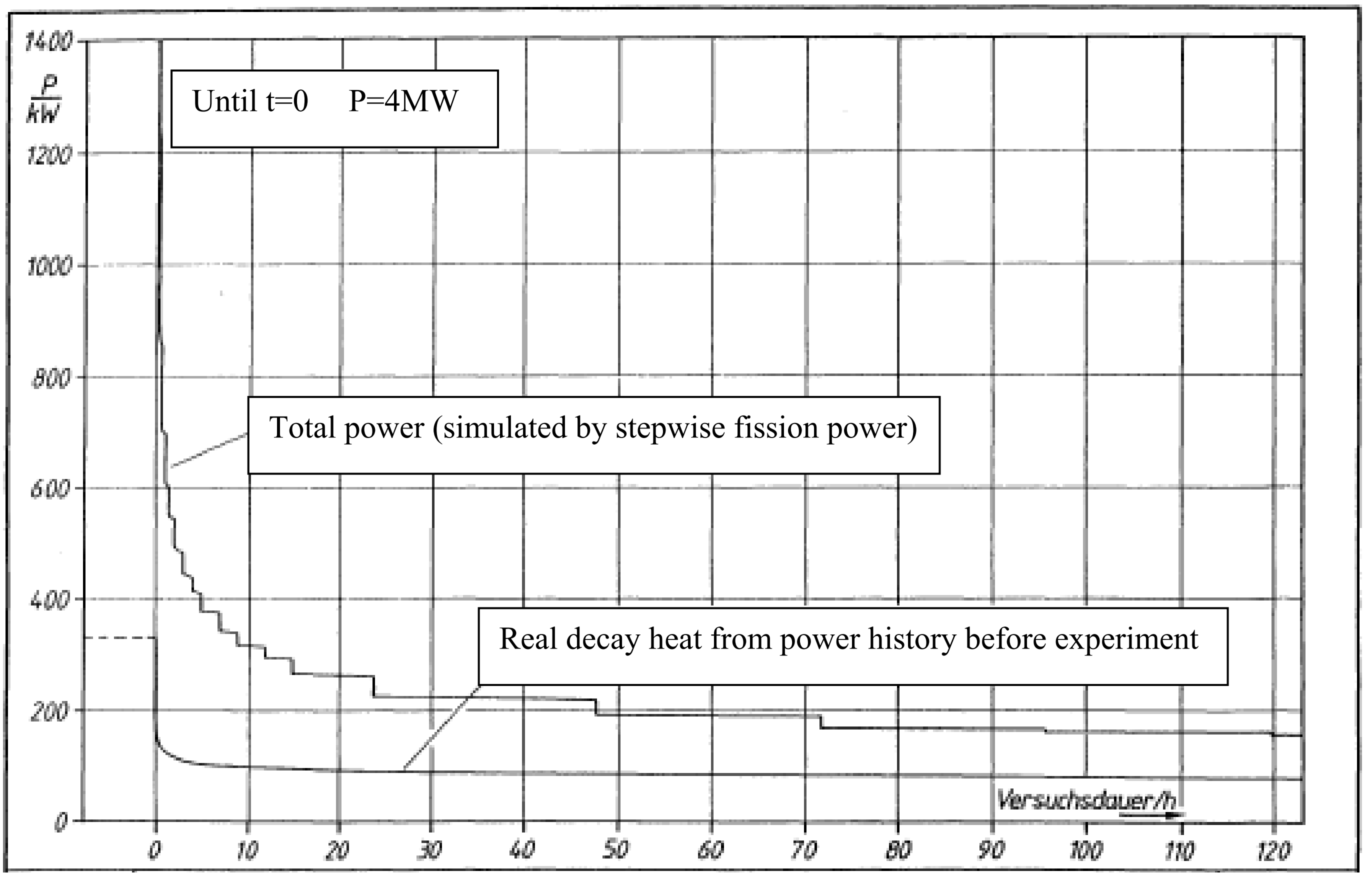

Simulation of the decay heat during LOCA experiment (date 14.10.1988)

Figure 19: Simulation of the decay heat during LOCA experiment

Table 12: Simulation of loss of coolant accident with AVR temperatures of reactor structures and coolant

No.	Description	Azimuth	Temperatur in °C																		
1		45°	543	650	700	740	780	818	840	850											
2	nose of control rod, core centre	135°	465	524	571	622	657	704	732	749	763	765	758	750	725	708	680	670	645	612	605
3		225°	608	710	750	780	810	840	855	860	860	850	840	805	775	755	730	718	695	670	650
4		45°	865	832	812	788	763	711	665	629	582	541	482	425	379	348	326	310	297	273	255
5	nose of control rod, above core	135°	862	820	805	780	739	705	645	570	540	490	430	370	320	280	270	241	220	191	180
6		225°	869	836	815	789	764	711	667	633	586	545	484	424	377	344	321	304	291	271	256
7	reflector inside		554	571	582	599	610	626	637	645	653	657	656	644	625	607	587	570	550	516	488
8	reflector middle	95°	545	550	559	569	578	586	610	612	621	630	630	620	602	584	568	551	535	501	472
9	reflector outside height of core centre		535	539	545	555	562	571	582	592	605	611	615	608	590	578	560	542	525	496	469
10	reflector inside	275°	502	525	535	545	550	562	570	580	588	591	592	585	571	558	540	525	510	488	465
11	reflector middle		533	535	547	556	566	581	592	601	612	617	620	612	599	581	563	545	531	500	477
12	bottom reflector	57,5°	203	218	229	241	248	272	292	308	338	360	403	441	473	490	495	499	497	493	471
13		177,5°	202	218	230	241	254	277	297	317	342	369	407	445	473	491	499	500	497	490	464
14		237,5°	207	220	231	242	253	275	297	316	342	366	406	444	474	491	498	498	494	478	457
15		295,5°	189	205	212	221	232	250	268	275	310	331	371	410	440	457	465	469	462	450	430
16	reactor casing, height of core centre	60°	276	281	289	290	291	295	300	300	306	311	320	323	322	320	320	315	302	269	250
17	height of core centre	350°	189	189	189	188	189	183	188	188	189	191	195	200	203	206	205	199	191	179	170
18	height of top reflector	60°	196	201	208	216	225	239	240	258	264	268	266	255	240	228	214	196	182	155	138
19	connection spherical calotte - flange	0°	152	151	150	151	151	150	148	148	148	148	146	142	138	131	126	122	121	122	112
20		120°	147	147	146	145	142	138	134	133	132	132	130	128	124	118	113	106	102	95	91
21		240°	147	148	146	144	142	137	132	126	122	120	116	114	110	107	107	112	111	110	109
22	roller bearing on support	65°	191	175	164	155	148	137	130	125	116	112	105	98	46	94	96	102	112	122	134
23	roller bearing on support inner reactor vessel	65°	124	121	119	111	108	101	94	90	86	82	78	73	70	68	65	62	62	65	68
24	pebble extraction tube	180°	198	197	198	199	201	204	207	209	213	217	227	242	260	274	284	290	292	290	281
25	bottom plate at pebble extraction tube	125°	163	182	181	183	183	180	182	180	180	180	180	182	189	198	204	209	209	215	207
26	between inner reactor vessel, height support	0°	148	149	152	154	157	162	168	172	178	184	188	187	182	176	172	167	160	146	134
27		120°	141	142	145	148	150	155	162	160	172	172	175	171	162	157	150	138	131	122	117
28	outer reactor vessel, height support	0°	52	53	53	53	53	53	53	52	53	53	51	51	50	49	48	47	46	45	44
29		120°	53	51	51	52	52	52	52	52	52	51	51	50	49	48	48	44	43	42	41
30	outer reactor vessel, upper spherical calotte	0°	93	94	94	94	95	94	93	93	93	93	92	90	87	84	81	79	78	76	69
31	outer reactor vessel, upper flange	120°	98	99	98	98	94	90	86	84	82	82	80	78	74	71	69	61	60	55	55
32	Gas temperature at blower	90°	183	163	157	151	150	145	139	134	128	122	112	104	98	94	92	91	89	87	83
33		270°	183	161	156	151	150	145	141	135	129	123	114	106	100	96	93	91	89	84	79
34	Gas temperature steam generator outlet 11	50°	130	109			69	66	65	60	63	62	63	62	62	61	72	61	62	61	62
35	Gas temperature steam generator outlet 2,1	170°	121	100	90	75	61	60	60	60	60	58	60	59	59	58	60	59	60	59	59
36	Gas temperature steam generator outlet 2,8	290°	121	100	91	80	65	60	62	62	62	61	60	60	60	60	60	60	60	60	60
37	cold gas temperature, height of core centre	120°	189	168	161	154	149	141	135	129	122	116	107	99	92	87	86	85	85	85	84
		Time/h	0	1	2	3	4	6	8	10	13	16	22	30	40	50	60	70	80	100	123

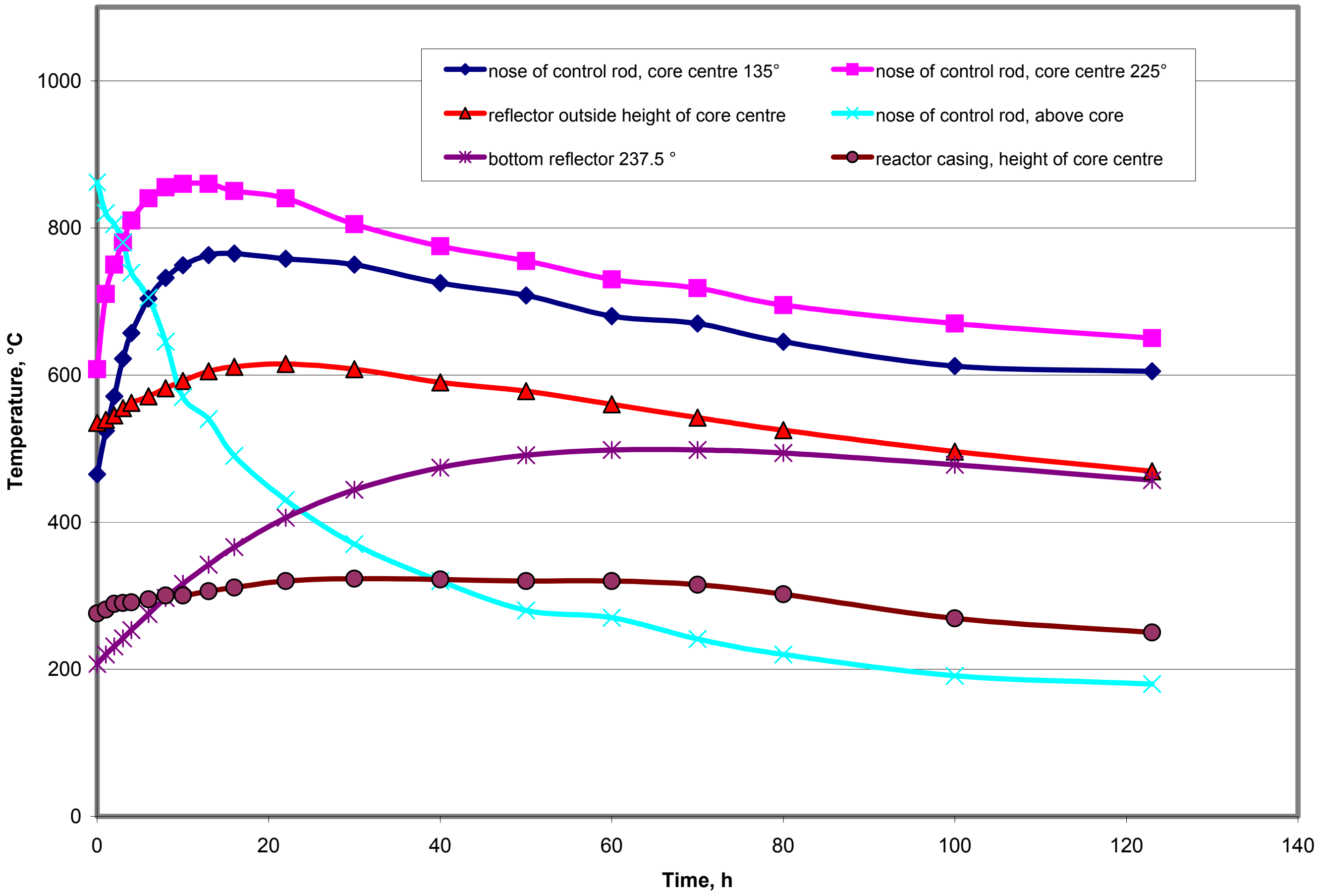

Figure 20: Temperatures at LOCA simulation experiment with AVR

Table 13: Rod position and reactivity at simulation of LOCA accident

Experiment Oct. 14th 1988	Position	
	Rod insertion [2]	reactivity ρ [3]
Time in h	in cm	in mNile
0 [1]	118	1250
1	98	756
2	87	546
3	79	415
4	73	334
5	68	279
6	66	254
7	63	225
8	62	216
9	62	216
10	63	225
11	64	234
12	65	244
14	68	284
16	73	334
18	78	409
20	82	463
22	86	523
24	89	586
26	94	681
28	98	756
30	101	826
35	108	980
40	112	1075
45	115	1170
50	119	1270
60	125	1450
70	129	1550
80	133	1690
90	137	1800
100	138	1840

[1] stationary state
[2] insertion measured from bottom reflector
[3] reactivity bound by inserted rods

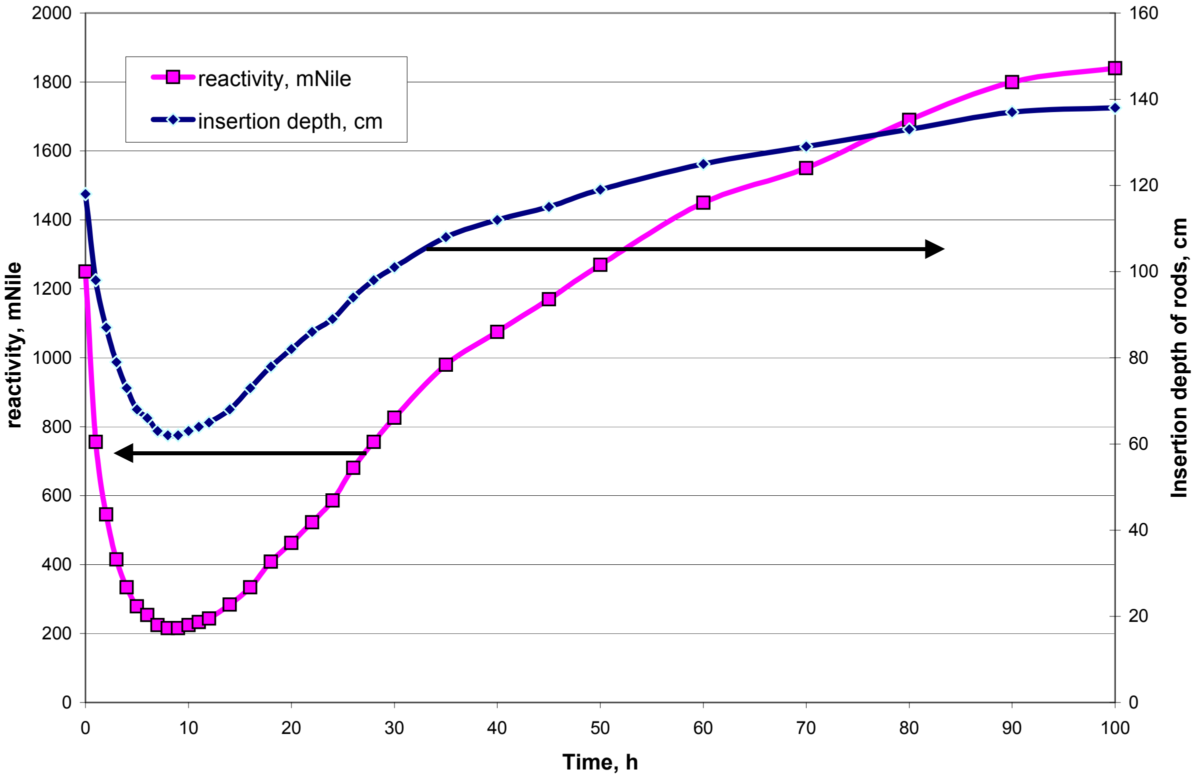

Figure 21: Rod position and reactivity at simulation of LOCA with AVR

Table 14: simulation of LOCA – data of steam generator

t min	$\dot{m}_{Spw}$* t/h	ϑ_{Spw} °C	ϑ_{Fd} °C	ϑ_{EK} °C	P_{DE} kW
0	25,5	130	256	203	3999
0,6					
1,2				203	
1,8			256	202	3999
2,4			255		3964
3,0			251	202	3827
3,6			246	201	3656
4,2			241	201	3487
4,8			237	200	3353
5,4			232		3186
6,0			229	200	3087
6,6	25,5		225	199	2956
7,2	25,1		220		2749
7,8	24,7		219	199	2673
8,4	24,2		217	198	2558
9,0	23,9		215	198	2465
9,6	23,5		214	197	2394
10,2	23,1	130	212	197	2295
10,8	22,7	129	211	196	2254
11,4	22,4		210	196	2196
12,0	22,0		209	195	2129
12,6	24,0	129	208	194	2292
13,2	26,2	128	208	193	2533
13,8	25,6		207	192	2443
14,4	24,9	128	207	190	2376
15,0	24,2	127	206	188	2308
15,6	23,5		205	185	2212
16,2	22,9		204	182	2127
16,8	22,2		203	179	2034
17,4	21,7	127	202	176	1961
18,0	21,0	126	201	173	1896
18,6	20,3		200	170	1808
19,2			199	168	1783
19,8			198	164	1758
20,4			196	163	1707
21		126	195	161	1682
24		125	183	155	1407
27	20,3	124	175	150	1234
30	20,4	123	169	148	1116
33	20,4	123	165	146	1017
36	20,5	122	162	144	973
39	20,4	121	161	144	967
42	20,5	120	159	143	947
45		119	158	143	947
60		112	150	135	919
75		108	144	130	869
78,6	20,5				
79,2	19,9				
90	19,9	102	140	125	889
105	20,1	99	135	120	850
120	20,3	96	130	115	809
135	20,3	92	125	112	784
150	20,4	86	121	108	835
165	20,5	79	117	104	910
180	20,6	74	113	100	937
195	20,7	70	107	93	893
210	19,9	67	102	88	811
225	19,9	64	98	84	787
240	20,0	61	94	80	767
255		60	92	78	744
270		60	89	75	674
285		58	86	73	651
300	20,0	57	84	72	627

t h	$\dot{m}_{Spw}$ t/h	ϑ_{Spw} °C	ϑ_{Fd} °C	P_{DE} kW
6	20,0	61	82	488
7			82	488
8		61	81	465
9		60	81	488
10		60	79	441
11		59	79	464
12		59	77	418
13		60		395
14			77	395
16			76	371
18			75	348
20			75	348
22			74	325
24			73	302
26			73	302
28			72	279
30				
32			72	279
34			70	232
36				
38				
40			70	232
45			69	209
50				
55				
60	20,0		69	209
65	20,2		68	187
70	20,0			186
75		60	68	
80		61	69	
85		60	68	186
90		61	68	162
95		58	66	186
100		60	67	162
105		61	69	186
110			68	162
115				
120			68	162
123	20,0	61	67	139

* approx. as ramp

t   time after shut down of blowers
$\dot{m}_{Spw}$ feed water flow
ϑ_{Spw} feed water temperature
ϑ_{Fd} steam generator temperature
ϑ_{EK} cooler temperature (before overheater)
P_{DE} steam generator power

Speisewasserdruck : stationär 80 bar
Versuch 84 bar

DE-Druckverlust : stationär 10 bar
Versuch 14 bar

Table 15: simulation of LOCA – interspace cooler data

Duration of experiment	Gas temperature		Temperature of coolant		Coolant flow 1)
	Inlet	outlet	Inlet	outlet	
in h	(W5.2.1)	(W5.2.2)	(W8.2.44a)	(W8.2.44)	in m^3/h
0 2)	135	36	31	34	4,5
2	128	36	31	33	|
6	108	35	30	32	|
10	|	34	28	30	|
14	|	33	26	28	|
20	108	31	25	27	|
40	105	27	20	22	|
60	93	26	18	20	|
80	82	25	|	19	|
100	|	|	|	|	|
123	82	25	18	19	4,5

1) coolant flow approx. constant (WB.1.72)
2) begin of simulation of accident

7 Literature

[1] "International Reactor Physics Experiment Evaluation Handbook" of the OECD/NEA data bank, 2006

[2] "AVR-Experimental High-Temperature Reactor - 21 Years of Successful Operation for a Future Energy Technology", 1990

[3] H. Werner : "HTR-2000 A simulation program system for power reactors."

[4] P. Pohl : "Compilation of measured data for the AVR dynamic experiments from 1st March until 5th March 1988 (in German), AZ: H5-X1 Pl/Ha/Bot, 1990" and

P. Pohl : "Simulation of loss of coolant accident at AVR, Compilation measured data for main experiment in Oct. 1988", AZ : H5-X1 Pl/Bot, 8 May 1989 and

P. Pohl : "Experimental report for the retried simulation of a loss of coolant accident at AVR in Oct. 1988" AVR-AN 27. Oct. 1988

[5] K. Krüger, Experimental simulation of a loss of coolant accident with the AVR reactor. Report Jül-2297 (1989)

Appendix 1: Structure of number density file for AVR fuel regions

For every fuel region of AVR (see core subdivision in Fig. 8) following information concerning the number densities are given :

i) description of data file (date)
ii) percentage of fuel type 1, 2, ..., 9 in region (see table 3 and 4)
iii) number densities of 77 nuclides (see table 3a) for every fuel type corresponding to burnup in core region at a distinct date, e.g. October 1985

The number densities are given in Atome/(FA.barn) for every FA type.

The participant of the benchmark should use the given data according to the features of the program system applied for the benchmark. The data file is written in ascii format as follows :

1) Description of data file including date of AVR status
2) NTYPE, NREG, NNUC (integers, format free)
   ... NTYPE number of FA-types (9)
   ... NREG number of core regions (139)
   ... NNVC number of Nuclides (77)
3) For every region J, J=1,2,..., NREG it follows :
3.1) (PART(i), i=1, NTYPE) Percentage of FA of type i
3.2) For every fuel assembly type i follows:
   (DENS(l,i,j), l=1, NNUC) Number densities of nuclide l in FA type i in region j in Atome/(FA.barn)

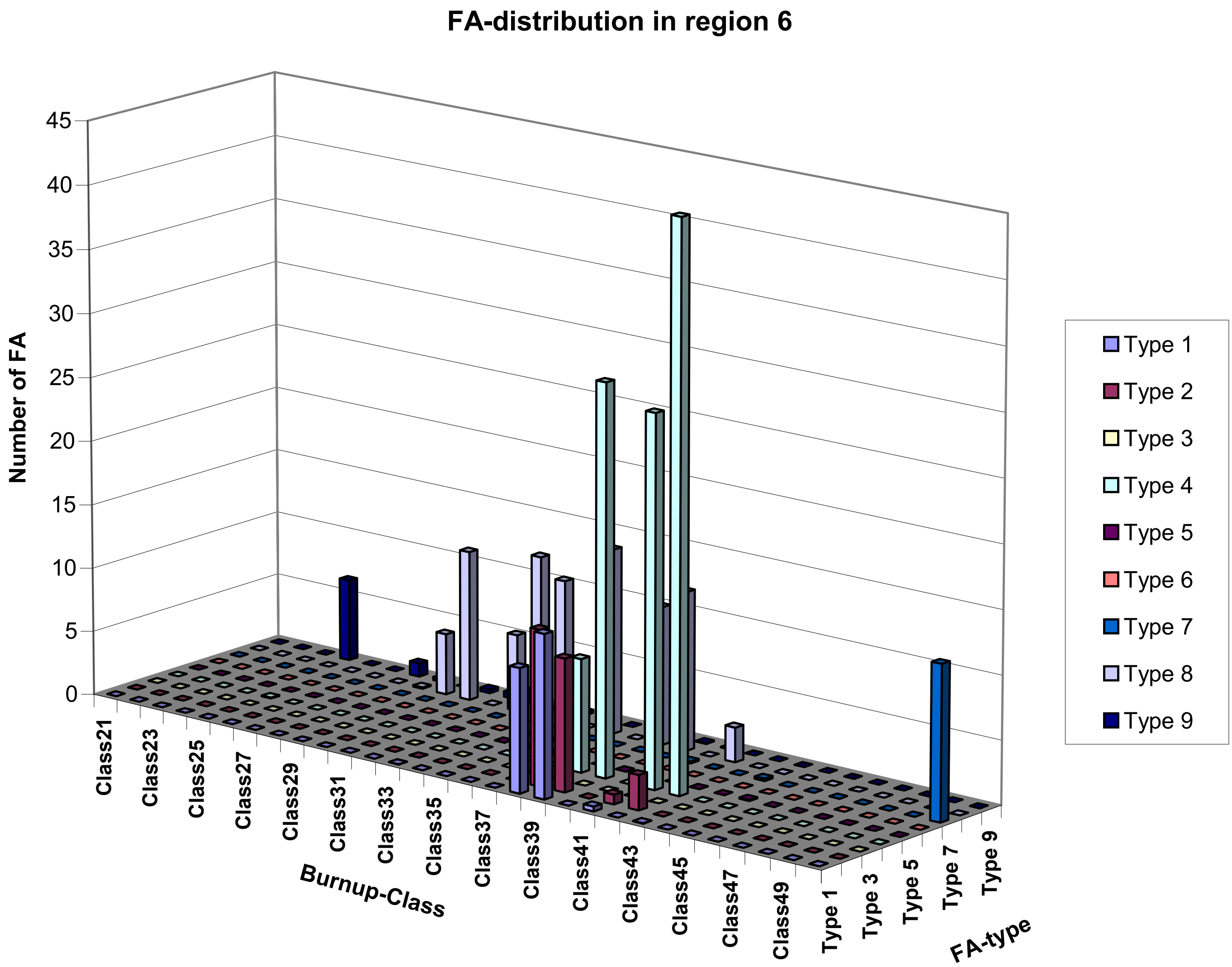

Figure 22: Distribution of different fuel element types in burnup region 6 (see Fig.8)